Published in Dalton Transactions, 2019, 48, 1976-1992

Available at : https://doi.org/10.1039/C8DT04813D

ARTICLE

Methimazolyl Based Diptych Bicyclo-[3.3.0]-Ruthenaboratranes

Chenxi Ma[a] and Anthony F. Hill*[,a]

Received 00th January 20xx,
Accepted 00th January 20xx

DOI: 10.1039/x0xx00000x

www.rsc.org/

The reactions [RuCl(R)(CO)(PPh_3)$_2$] (R = CH=CHPh, Ph) with Na[H_2B(mt)$_2$] (mt = *N*-methyl-2-mercaptoimidazolyl) transiently provide [Ru(R)(CO)(PPh_3){κ^3-*H,S,S'*-H_2B(mt)$_2$}] which each evolve to the ruthenaboratrane [Ru(CO)(PPh_3)$_2${κ^3-B,S,S'-BH(mt)$_2$}]*(Ru→B)*[8]. The phosphine ligands may be selectively replaced to provide the complexes [Ru(CO)(L)(PPh_3){κ^3-B,S,S'-BH(mt)$_2$}] (L = CO, PMe_2Ph) and [Ru(CO)L$_2${κ^3-B,S,S'-BH(mt)$_2$}] (L = PMe_2Ph, $P(OMe)_3$, L$_2$ = Z-Ph_2PCH=$CHPPh_2$) with, in each case, retention of the ruthenium-boron dative bond.

Introduction

The term 'metallaboratrane' has been coined to draw analogy between the first such compound [Ru(CO)(PPh_3){κ^4-*B,S,S',S''*-B(mt)$_3$}] (mt = *N*-methylmercaptoimidazolyl),[1-2] and Brown's boratrane B(OCH_2CH_2)$_3$N, given that both *tricyclo*-[3.3.3.0] cage structures include a *trans*-annular dative (polar covalent,[4,5] M→B *cf.* N→B) bond. (Chart 1).

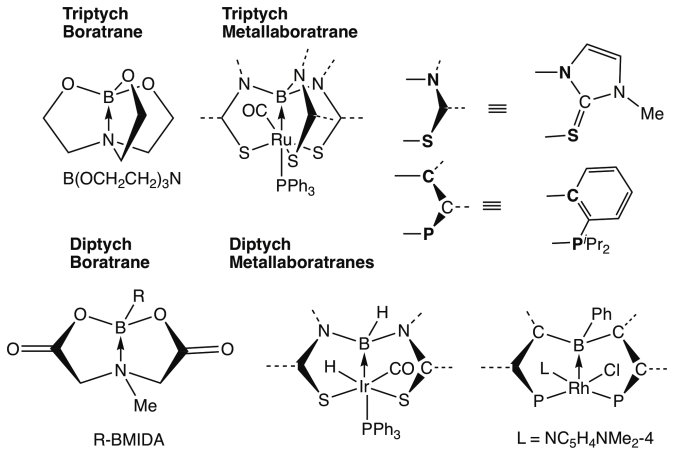

Chart 1. (a) Triptych and (b) Diptych boratranes and metallaboratranes.

A large number of *tricyclo*-[3.3.3.0] metallaboratranes are now known based on cages in which the buttresses are variants on the original *N*-heterocycle (mt)[6] or alternatively, 2-phosphinoaryl bridges as pioneered by Bourissou.[7] It might be argued that the presence of the *trans*-annular M→B interaction is in part a simple corollary of the geometric constraints imposed by the cage. Indeed, a recent attempt to assay the strength of this interaction through correlation of structural and spectroscopic data for an extensive series of the tri-buttressed ('triptych') ruthenaboratranes [Ru(CO)L{κ^4-*B,S,S',S''*-B(mt)$_3$}] (L = PPh_3, CO, CN^{t}Bu, $CNC_6H_2Me_3$, PMe_3, PMe_2Ph, $P(OMe)_3$, $P(OPh)_3$, PCy_3) was generally unsuccessful,[8] concluding that subtleties in the Ru→B bonding might be outweighed by inter- and intramolecular non-bonding interactions and cage strain.

Dibutressed ('diptych') boratranes are not only well-known[9] but also enjoy practical application in organic synthesis, most notably the B(O_2CCH_2)$_2$NMe group found in BMIDA borates.[10] Within the field of metallaboratrane chemistry, a number of dibuttressed 'diptych' metallaboratranes have been isolated (Chart 1), however these remain comparatively rare, based either on *N*-heterocyclic buttresses[11] or Bourissou's 2-phosphinoaryl system.[7,12] To these may be added a small number of *potentially* triptych systems in which one buttress, however, remains pendant, at least in the solid state.[11a,13] The majority of these involve the heavier (4d or 5d) group 9 and 10 metals. A recurrent feature of the Ar-B($C_6H_4PR_2$)$_2$ (R = ^{i}Pr, Ph; Ar = Ph, $C_6H_2Me_3$) system, in particular for 3d metals Fe, Co and Ni, is the η^2-*B,C(ipso)* or 'η^3-*B,C,C'*-bora-allyl' type coordination[12a-c,e] of the B-aryl group. This is reminiscent of η^3-benzyl ligands, and provides a means by which coordinative unsaturation at the metal may be alleviated. Diptych *bicyclo*-[3.3.0] metallaboratranes are of interest in that the metal-boron interaction is not constrained within the more restrictive *tricyclo*-[3.3.3.0] triptych geometry, allowing more confidence in interrogating the nature of the M→B bond. Furthermore, the more exposed M→B bond has been found to play a non-innocent role in the activation of diatomic ligands such as CS,[14] H_2,[12a,c] CO[12a] and N_2.[12e]

Given that the majority of diptych metallaboratranes have emerged within groups 9 and 10, with the only group 8 examples being those based on Peters' [Fe(CO)$_n${BPh($C_6H_4P^iPr_2$-2)$_2$}]$^{x-}$(n = 2,3; x = 0,1,2) ferraboratranes,[12a-f] we have now revisited the archetypal zerovalent[5] ruthenium system to establish whether methimazolyl diptych ruthenaboratranes might also be viable.

[a] Research School of Chemistry, Australian National University, Acton, Canberra, A.C.T., Australia.

†Electronic Supplementary Information (ESI) available: Selected characterisational spectra; Crystallographic information files CCDC 1881115-1881118 and 1881121 - 1881125 relate to compounds discussed herein.

Results and Discussion

Synthesis and Reactivity

The triptych ruthenaboratrane [Ru(CO)(PPh$_3$){κ^4-*B,S,S′,S″*-B(mt)$_3$}] (**1a**) arose from the reactions of [RuCl(R)(CO)(PPh$_3$)$_2$] (R = Ph,[15] CH=CHPh[16]) with Na[HB(mt)$_3$],[1a] which were presumed to proceed *via* the complexes [Ru(R)(CO)(PPh$_3$){HB(mt)$_3$}] (R = Ph **2a**, CH=CHPh **2b**) although these could not be isolated. In contrast the reactions of [RuHCl(CO)(PPh$_3$)$_3$] with either Na[HB(mt)$_3$] or Na[H$_2$B(mt)$_2$][17] afforded the stable hydrido complexes [RuH(CO)(PPh$_3$){κ^3-*H,S,S′*-HBR(mt)$_2$}] (R = H **2c**, mt **3**).[1b,18] The κ^3-*H,S,S′* coordination mode has in the interim been found to be favourable for a wide range of transition metals and is especially prevalent within the chemistry of ruthenium.[18,19] In extending studies on this mode of coordination, we recently described the series of complexes [RuR(CO)(PPh$_3$){κ^3-*H,S,S′*-H$_2$B(mt)$_2$}] (R = H **2c**, Cl **4a**, SeH **4b**, SePh **4c**, SiCl$_3$ **4d**, SiMe$_3$ **4e**, BO$_2$C$_6$H$_4$ **4f**),[18] none of which underwent the B–H activation step required for the installation of the metallaboratrane cage. In contrast, whilst the σ-organyl derivatives [RuR(CO)(PPh$_3$){κ^3-*H,S,S′*-H$_2$B(mt)$_2$}] (R = Ph **4g**, CH=CHPh **4h**) could be spectroscopically observed (See Experimental), they eluded isolation due to their spontaneous evolution into what we now identify as the diptych ruthenaboratrane [Ru(CO)(PPh$_3$)$_2${κ^3-*B,S,S′*-BH(mt)$_2$}]*(Ru→B)*[8] (**5**) (Scheme 1, Figure 1).[20]

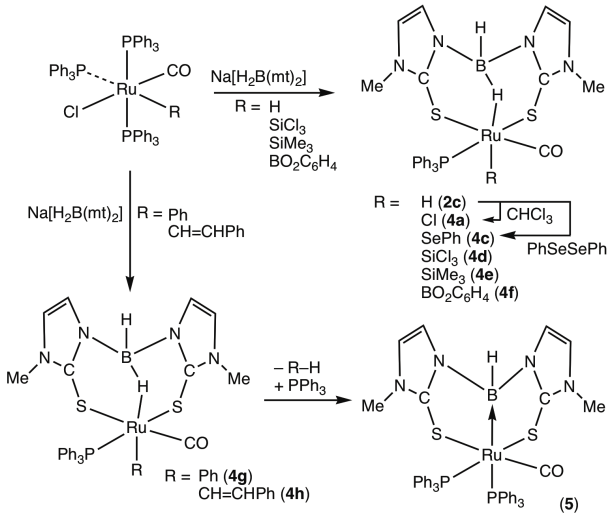

Scheme 1. Synthesis of a diptych ruthenaboratrane

The initial synthesis of **5** involved employing the phenyl precursor [RuCl(Ph)(CO)(PPh$_3$)$_2$] which also resulted in the formation of a side product [Ru(Ph)(CO)(κ^2-N,S-mt)(PPh$_3$)$_2$] (**6**) and its removal by extensive washing with diethyl ether somewhat compromised the isolated yield of **5** (34%). The complex **6** has been described previously by Wilton-Ely including a crystallographic study of a dichloromethane solvate.[21] The determination of the crystal structure of unsolvated **6** is presented in the experimental section but calls for no further comment. Given that the synthesis of [RuCl(Ph)(CO)(PPh$_3$)$_2$] requires the undesirable use of diphenyl mercury, an alternative more convenient and higher yielding synthesis of **5** was developed directly from *mer*-[RuHCl(CO)(PPh$_3$)$_3$] (**7**). The reaction of **7** with ethynylbenzene to afford the *trans*-β-styryl complex [RuCl(CH=CHPh)(CO)(PPh$_3$)$_2$] is rapid and essentially quantitative,[16] such that successive treatment of **7** with HC≡CPh and Na[H$_2$B(mt)$_2$] returned **5** in 61% yield (3 g scale, 'one pot').

The low symmetry of complex **5** (C_1) follows from the appearance of two distinct methyl resonances in the ^{1}H NMR spectrum (δ_H = 3.07, 3.33), as well as four imidazolyl peaks (δ_H = 6.04, 6.15, 6.50, 6.58 d x 4, $^3J_{HH}$ = 1.8 Hz) indicating the chemical inequivalence of the two methimazolyl arms, which was also evident from ^{13}C{^{1}H} NMR data. Despite the broadening of the borohydride resonance by the quadrupolar boron nuclei (^{10}B and ^{11}B), the BH resonance was identified at δ_H = 4.07 (h.h.w. = 209 Hz). A single boron resonance (^{11}B{^{1}H}: δ_B = 4.12) was observed in a region consistent with four-coordinate metal-bound boron.[1,2] The two phosphine environments were manifest as resonances at δ_P = 19.3 and 52.7, where the broadness of the latter resonance was indicative of coordination *trans* to the boron. The composition of complex **5** was further supported in the HR-ESI(+ve ion, MOH matrix) mass spectrum with a peak corresponding to a [M–CO+OMe]$^+$ adduct (*m/z* = 895.1592).

The formulation of **5** was confirmed by an X-ray crystallographic study, the results of which are summarised in Figure 1. This reveals a distorted octahedral coordination at ruthenium and distorted tetrahedral geometry about boron with angles in the range of 104.7(12)–123.2(13)°. The Ru1–B1 bond length of 2.2463(16) Å is somewhat longer than found in the corresponding triptych analogue **1a** (2.161(5) Å; Δ = 17 e.s.d.), falling outside the range previously observed for Ru→B bonds (2.157(6) - 2.184(6)Å).[1,8]

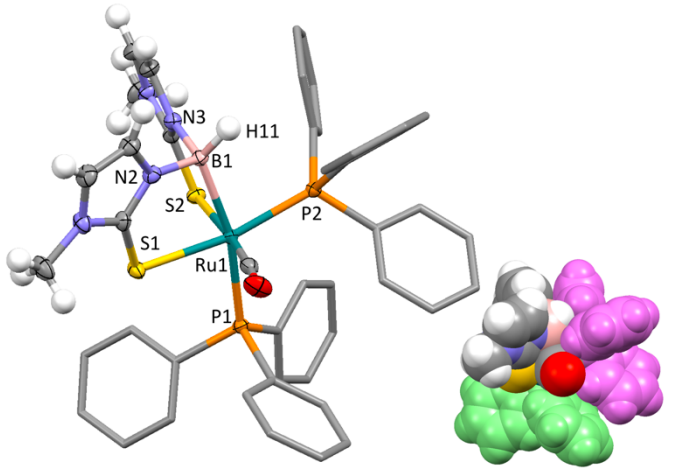

Figure 1. Molecular structure of **5** in a crystal of **5**.Et$_2$O (Hydrogen atoms and Et$_2$O solvent omitted, phenyl groups simplified, 50% displacement ellipsoids). Data collected using both Mo-Kα and Cu-Kα radiation Selected bond lengths (Å) and angles (°) derived from Cu-Kα data: B1–Ru1 2.2463(16), B1–H1 1.17(2), Ru1–P1 2.4766(4), Ru1–P2 2.3045(4), Ru1–C1 1.8336(16), H1–B1–Ru1 123.3(13), N2–B1–H1 104.7(12), N3–B1–H1 106.1(12), B1–Ru1–P1 166.36(4), B1–Ru1–P2 84.13(4), P1–Ru1–P2 108.061(13). Inset = Space filling representations showing PPh$_3$ ligands in lilac and green.

Notably, the two Ru–P bonds are very significantly different in length (430 e.s.d.), where the phosphine *trans* to boron exhibits a far longer bond than that *trans* to sulfur. The comparatively pronounced *trans* influence of M→B bonds has been noted previously for the complexes [Rh(PMe$_3$)$_2${B(mt)$_3$}]$^+$, [PtI$_2${B(mt)$_3$}] and [Fe(CO)$_2${B(mt^{tBu})$_3$}] wherein the boron and

one thione donor are *trans* to identical σ-donor (PMe_3),[22] (σ+π) donor (iodide)[23] or π-acceptor (CO)[24] ligands.

The formation of a minor side product (**8**, *ca* 1%) was observed to accompany the isolation of **5** when the 'one-pot' procedure was used and whilst this was only isolated in sufficient quantity for crystallographic characterisation, details are included here as they provide two relevant points of interest. The product was identified as the alkynyl complex [Ru(C≡CPh)(CO)(PPh_3){κ³-*H,S,S'*-$H_2B(mt)_2$}] (**8**, Figure 2) which is akin to the complexes **2c** and **4a-f** but distinct from **4g** and **4h** in being a thermally stable σ-organyl derivative that does not evolve to **5**.

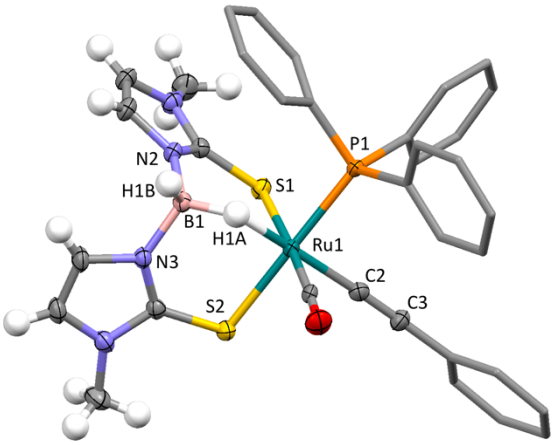

Figure 2. Molecular structure of **8** in a crystal of **8**.$CHCl_3$ (Hydrocarbon hydrogen atoms and $CHCl_3$ solvent omitted, phenyl groups simplified, 50% displacement ellipsoids). Selected bond lengths (Å) and angles (°): B1···Ru1 2.740(2), B1–H1 1.24(4), B1–H2 1.19(4), Ru1–H1 1.74(4), Ru1–P1 2.3228(6), Ru1–C1 1.864(2), Ru1–C2 2.028(3), C2–C3 1.200(4), C3–C4 1.448(3), B1– H1–Ru1 134(3), H1–Ru1–C2 173.3(14), S2–Ru1–P1 176.25(2), S1–Ru1–P1 87.20(2), S1–Ru1–S2 89.82(2).

Notably, treating **5** with an excess of ethynylbenzene does not lead to formation of **8** under the conditions in which it was first isolated. This leaves two possible mechanistic routes to **8**, both of which involve the occasionally observed cleavage of ruthenium alkenyls by terminal alkynes to provide σ-alkynyl derivatives, a process that underpins the catalytic dimerization of terminal alkynes to provide butenynes.[25] The first possibility is that a small amount of unreacted [RuHCl(CO)(PPh_3)$_3$] remained at the time Na[$H_2B(mt)_2$] was added (the alkyne hydroruthenation is also a reversible process), being converted to **2c** followed by alkyne hydrometallation to generate **4h** which then undergoes (net) σ-metathesis with ethynylbenzene to generate the alkynyl complex **8**. This may be excluded because it could be shown in separate experiments that pre-isolated **2c** is unreactive towards HC≡CPh under these conditions. Under more forcing conditions, with an excess of HC≡CPh, the hydride precursor [RuHCl(CO)(PPh_3)$_3$] affords [RuCl{C(C≡CPh)=CHPh}-(CO)(PPh_3)$_2$],[26] which is an effective alkyne dimerization catalyst.[27] The yet to be isolated species 'RuCl(C≡CPh)(CO)(PPh_3)$_n$' (n = 2,3) being plausible resting states that might react with Na[$H_2B(mt)_2$] to afford **8**. The mild conditions under which **8** forms would seem to argue against this. The final mechanism, which we consider the most plausible, involves a reaction of **4h** with HC≡CPh to provide **8** and styrene, in a process that operates to a very modest extent in competition with the metallaboratrane formation.

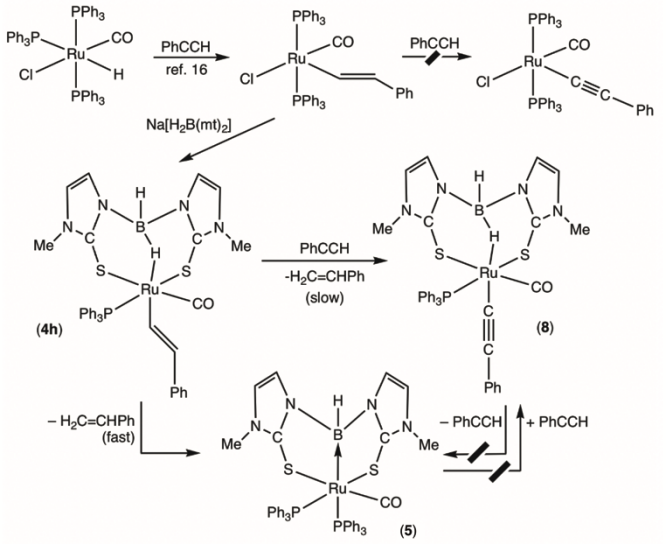

Scheme 2. Mechanism conjecture to account for the formation of a borato alkynyl complex **8**.

The structural features of **8** (Figure 2) correlate well with those reported for the analogous complexes **2c** and **4a**-**4f** and call for little comment other than to note that the Ru···B separation of 2.740(2)Å falls within the range previously observed (*cf.* 2.651–2.897 Å), as does the less precisely determined B–H–Ru angle of 134(3)° (*cf.* 128–138°).[18] The Ru–C and C–C bonds are also well within the ranges observed for the copious structural data available for octahedral ruthenium(II) alkynyls.

The potential of the M→B association to engage directly in reactions has been long of interest. In particular, the question of interconversion between coordination modes κ³-*B,S,S'* and κ³-*H,S,S' via* hydride migration from the metal centre was first demonstrated when the platinaboratrane [PtH{P(C_6H_4Me-4)$_3$}{B($mt)_3$}]Cl was shown to undergo phosphine substitution by PMe_3 or PEt_3 accompanied by reconstitution of the κ³-*H,S,S'*-HB($mt)_3$ coordination.[25] In the interim, further examples of hydrogenation of M→B bonds have emerged,[11h,i,12d,f,i,13b] some of which involve heterolytic cleavage of dihydrogen itself to generate metal hydride (M–H$^{\delta+}$) and boron-hydride (M–H$^{\delta-}$) units. Taken together, the complexes [Co(H_2){κ⁴-*B,P,P',P''*-B($C_6H_4P^iPr_2$-2)$_3$}][12e] and [MH(CO)$_x${κ³-*H,P,P'*-HB($C_6H_2Me_3$)($C_6H_4P^iPr_2$)$_2$}] [M = Ni, x = 0;[12c] M = Fe x = 2[12a]) provide an elegant indication of the subtleties at play along the dihydrogen cleavage trajectory.

As noted above, **5** fails to react with ethynylbenzene to afford **8** and in a similar manner, no reaction is observed between **5** and $HBO_2C_6H_4$ (HBCat), dihydrogen, or pentamethylcyclopentadiene even though plausible products of such reactions [RuH(CO)(PPh_3){$H_2B(mt)_2$}] (**2c**), [Ru(BCat)(CO)(PPh_3){$H_2B(mt)_2$}] (**4f**)[18] and [Ru{$H_2B(mt)_2$}(η-C_5Me_5)] are all known and stable.[19h] In contrast, treating **5** with one equivalent of hydrogen chloride results in extensive decomposition and degradation of the cage such that a mixture of products was obtained within one hour (distribution invariant

over 24 hours) with complete consumption of **5**. Numerous resonances were observed in the $^{31}P\{^{1}H\}$ NMR spectrum (δ_P = 19.1, 28.1, 35.7, 45.2, 50.0 and 55.2) none of which predominated or corresponded to the anticipated chloro complex [RuCl(CO)(PPh_3){$H_2B(mt)_2$}] (**4a**: δ_P = 36.3; δ_H = –18.11; δ_B = –7.36).[18] Attempts to identify the products formed through crystallisation of the crude mixture from chloroform/n-pentane afforded complexes **9** and **10** as a mixture, which could be further purified to exclusively isolate **10** (Scheme 3).

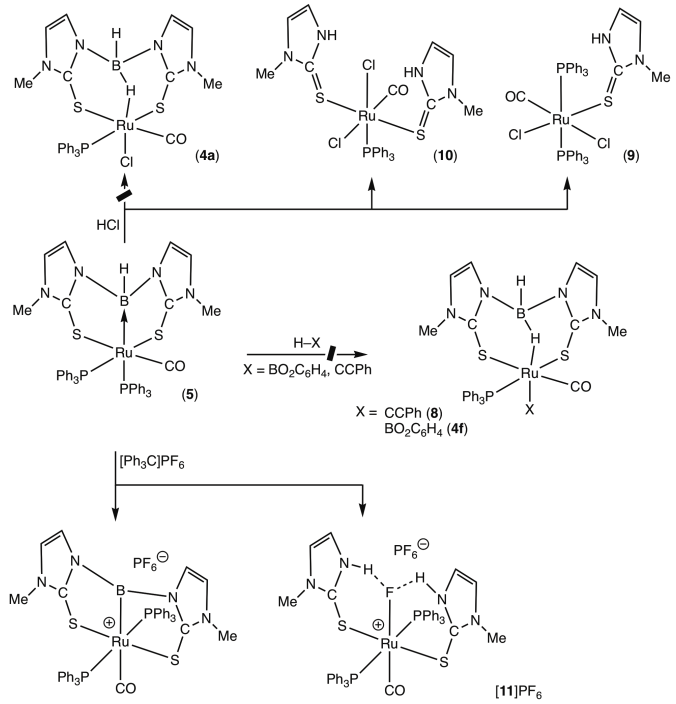

Scheme 3. Metallaboratrane degradation processes.

The formulations of complexes **9** (Figure 3) and **10** (Figure 4) were confirmed by X-ray diffraction studies, however unequivocal syntheses were not explored due to their rather mundane nature.

The key bond lengths and angles of **9** and **10** are consistent with other reported structures of thione bound N-methyl-2-mercaptoimidazole ligands on Ru(II) centres.[21,29] For example, the Ru–S bond lengths of 2.3845(6) Å in **9** and 2.4128(12), 2.4240(11) Å in **10** show little deviation from the range established for published complexes (2.391–2.553 Å). Similarly, the Ru1–S1–C2 angle of 115.59(9)° in **9** or 112.20(16) and 112.46(14)° for **10** lie within the previously observed range 107–119°. The molecular structure of **10** depicted in Figure 4 is consistent with spectroscopic data. The IR spectrum shows one CO absorption (1961 cm^{-1}) while the symmetric mutually *trans* coordination of two methimazole groups was inferred through ^{1}H NMR integration relative to the triphenylphosphine co-ligand. The triphenylphosphine ligand of isolated complex **10**

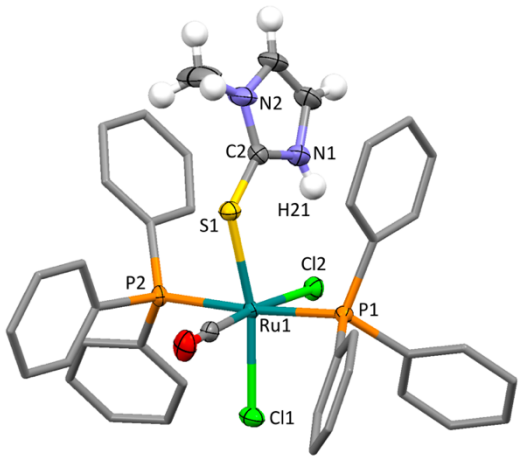

Figure 3. Molecular structure of **9** in a crystal of **9**.$CHCl_3$ ($CHCl_3$ solvent omitted, phenyl groups simplified, 50% displacement ellipsoids). Selected bond lengths (Å) and angles (°): Ru1–Cl1 2.4351(6), Ru1–Cl2 2.4841(6), Ru1–S1 2 .3845(6), Ru1–P1 2.3982(6), Ru1–P2 2.4239(6), Ru1–C1 1.833(3), Ru1–S1–C2 115.59(9), S1–Ru1–Cl1 165.87(2), P1–Ru1–P2 175.03(2), C1–Ru1–Cl2 174.40(8).

gives rise to a resonance at δ_P = 45.1 and by a process of elimination from the spectrum of the crude mixture, **9** was identified as being responsible for the resonance at δ_P = 19.1. The formulations of both complexes were further confirmed by HR ESI(+ve ion) mass spectrometry, with isotopic clusters corresponding to $[M - Cl]^+$ at *m/z* = 803.0754 for **9** and 655.0102 for **10**.

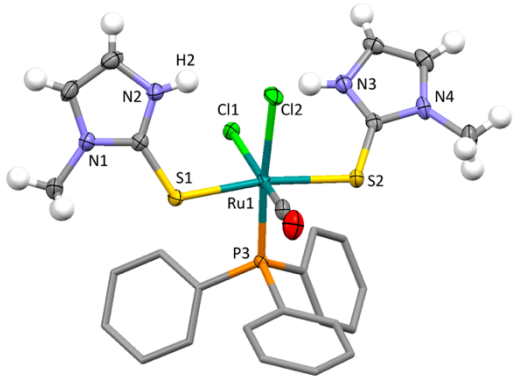

Figure 4. Molecular structure of **10** in a crystal of **10**.$CHCl_3$ (Hydrocarbon hydrogen atoms and $CHCl_3$ solvent omitted, phenyl groups simplified, 50% displacement ellipsoids). Selected bond lengths (Å) and angles (°): Ru1–Cl1 2.4804(11), Ru1–Cl2 2.4763(11), Ru1–S1 2.4128(12), Ru1–S2 2.4240(11), Ru1–P1 2.3110(11), Ru1–C1 1.827(5), Ru1–S1–C11 112.20(16), Ru1–S2–C15 112.46(14), S1–Ru1–S2 169.21(4), P1–Ru1–Cl2 175.58(4), C1–Ru1–Cl1 170.99(14).

The platinaboratrane [Pt(PPh_3){κ^4-*B,S,S′,S″*-$B(mt)_3$}]*(Pt→B)*[10] undergoes oxidative addition with Br_2 or I_2 to generate Pt(II) complexes [PtX_2{κ^4-*B,S,S′,S″*-$B(mt)_3$}]*(Pt→B)*[8] (X = Br, I) with retention of the Pt→B bond.[28] In contrast, both the ferraboratrane [$Fe(CO)_2${$B(mt^{tBu})_3$}][24] and nickelaboratrane [NiBr{$B(mt^{tBu})_3$}][30] react with oxidants with rupture of the metal-boron bond and formation of B-functionalised tris(mercaptoimidazolyl)borate ligands. The reactions of **5** with either elemental bromine or iodine proved to be complex (> 10 products), with no single product predominating according to spectroscopic analysis (^{31}P NMR) of the crude reaction mixture or samples subjected to fractional crystallisation. Group 8

(M→B)[8] metallaboratranes upon oxidative addition would be expected to provide d^6 metal centres, *i.e.*, devoid of a pair of electrons housed in an orbital of metal-ligand σ-symmetry and therefore unable to sustain a dative bond to boron. In the case of Parkin's *(Fe→B)*[8] system,[24] which is able to presumably traverse single-electron transfer radical pathways more easily than ruthenium, addition of halogens across the Fe→B bond is the preferred outcome. Owen's report on the group 10 diptych metallaboratranes [M{$BH(mp)_2$}(PPh_3)] *(M→B)*[10] (M = Pt, Pd; mp = 2-mercaptopyidyl), suggests a fine balance between the coordination flexibility of the "$BH(mp)_2$" group.[11e] The "$BH_2(mp)_2$" unit typically coordinates facially, however in these metallaboratranes the nearly *trans*-disposed sulfurs exhibit more meridional-like κ^3-*B,S,S'* coordination (S–M–S = 161.14(3) Pt, 158.88(2)° Pd). Inspired by this result, **5** was treated with hydride abstractor [CPh_3][PF_6] to assess the potential of **5** to relax to meridional coordination upon boron hydride abstraction. Within two hours, the solution IR spectrum (THF) indicated a significant shift of the ν_{CO} band from 1899 cm^{-1} in **5** to 1931 and 1972 cm^{-1}, consistent with the conversion of a neutral to cationic complex. The conspicuous absence of a BH stretching band was also noted in the IR spectrum. Both the ^1H and $^{31}P\{^1H\}$ NMR spectra revealed broad resonances. In the crude $^{31}P\{^1H\}$ spectrum, the dominant product was identified at δ_P = 39.6 accompanied with distinct resonances corresponding to PF_6 (δ_P = –142.9) and free PPh_3. The broadness of the latter may imply the occurrence of rapid exchange processes. The resonance at δ_P = 39.6 persisted following purification through washing with diethyl ether. Attempts to identify the product through X-ray diffraction analysis of crystals obtained from slow evaporation of a benzene/n-pentane solution afforded the salt [RuF(Hmt)$_2$(CO)(PPh_3)$_2$]PF_6 [**11**]PF_6 (Scheme 3, Figure 5).

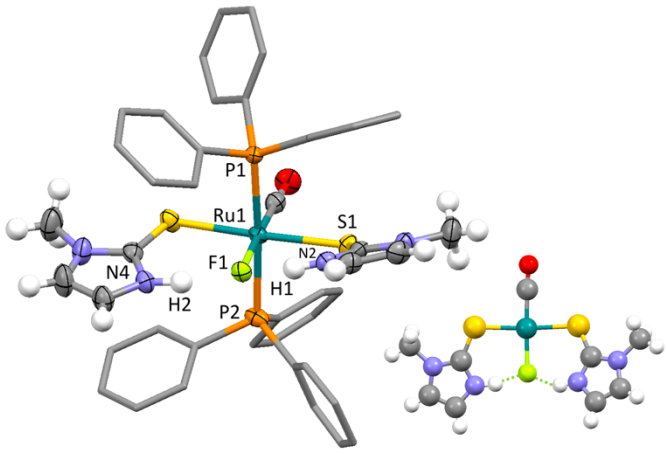

Figure 5. Molecular structure of [**11**]$^+$ in a crystal of [**11**]PF_6.C_6H_6 (benzene solvent and counter anion omitted, aryl hydrogen atoms omitted, phenyl groups simplified, 50% displacement ellipsoids). Selected bond lengths (Å) and angles (°): Ru1–F1 2.098(2), Ru1–S1 2.4338(10), Ru1–S2 2.4238(11), Ru1–P1 2.3970(9), Ru1–P2 2.4277(10), Ru1–C1 1.818(4), F1–Ru1–C1 177.70(15), S1–Ru1–F1 91.60(7), S2–Ru1–F1 92.30(7). Inset = view normal to the P1–Ru1 vector illustrating bifurcated NH···F···HN hydrogen bonding.

The cation of this salt features a terminal ruthenium fluoro ligand, the coordination of which is stabilised by bifurcated hydrogen bonding to two N-H groups from adjacent Hmt co-ligands (NH···F = 1.627, 1.764 Å). The fluoride is coordinated *trans* to the carbonyl ligand, as invariably observed for octahedral ruthenium fluoro-carbonyl complexes, presumably to maximise captodative interactions between the π-donor and π-acidic characters of the two ligands. The Ru–F distance of 2.098(2) Å lies within the range established by simple octahedral ruthenium complexes, despite the intramolecular hydrogen bonding.[31]

In contrast to the analogous **1a** which carries only one triphenylphosphine, the two triphenylphosphines within complex **5** each present potential sites for substitution and the *cis* disposition of these results in some inter-ligand repulsion which presumably also contributes to steric impetus in addition to the now recognised *trans* influence of M→B interactions. Accordingly, this aspect was investigated through ligand substitution reactions. Facile and clean substitution of triphenylphosphine was achieved by passing CO through a solution of **5** in THF for 15 minutes to selectively yield the symmetrical *cis*-dicarbonyl complex [$Ru(CO)_2(PPh_3)$\{κ^3-*B,S,S'*-$BH(mt)_2$\}] (**12**), with no evidence for the asymmetrical isomer **12x** (Scheme 4).

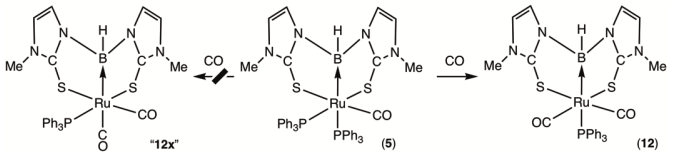

Scheme 4. Metallaboratrane carbonylation.

The reaction proceeded with increased symmetry (C_1 to C_s) as inferred from the ^1H NMR spectrum, manifest by the replacement of the two distinct methyl resonances in **5** by one resonance in **12** (δ_H = 3.43). The four independent olefinic proton resonances for **5** similarly simplified to two environments at δ_H = 6.62 and 6.69 [**ABCD** to **AA'BB'**]. The $^{13}C\{^1H\}$ NMR spectrum contained fewer resonances, as expected for C_s **12** compared to C_1 **5**, most notably, the appearance of a single carbonyl resonance (δ_C = 202.9, d, $^2J_{CP}$ = 2.4 Hz). Notably, only one phosphine environment was present in the $^{31}P\{^1H\}$ NMR spectrum of **12** (δ_P = 20.1), the broadness of which is consistent with coordination *trans* to the boron. The spectrum measured *in situ* included a resonance due to liberated PPh_3 which was sharp, confirming that exchange with the coordinated PPh_3 did not occur on the $^{31}P\{^1H\}$ NMR timescale (161 MHz at 25 °C). Furthermore, an absence of the resonance at δ_P = 52.7 corresponding to the phosphine of **5** trans to sulfur suggested replacement at this position by the CO ligand. Replacement of one phosphine by CO was further confirmed by IR spectroscopy, which showed two ν_{CO} associated bands (CH_2Cl_2: 1913, 1984 cm^{-1}).

The X-ray diffraction analysis of single crystals of **12**.$CHCl_3$ shown in Figure 6 was consistent with the symmetrical formulation inferred from spectroscopic data. In contrast to **5**, a space-filling diagram of **12** reveals less steric encumbrance about the equatorial plane occupied by the two CO ligands. Nevertheless, it is noteworthy that the carbonyl ligands appear to be displaced towards the Ru1-B1–H1 unit, a result that we attribute to an inter-ligand interaction in which this electron rich group donates into the CO π* orbitals. The mitigation of steric congestion associated with replacement at the equatorial

phosphine by CO is expected to be greater than at the (BRu) axial position, which may provide a rationale for the observed regioselectivity. In addition, the introduction of π-acidic CO is electronically favourable in further relieving the electron density at the π-basic electropositive Ru(0) metal centre. Certainly, location of the two strongest π-acids (CO) *trans* to the two strongest π-donors (mt) would be expected to maximise π-captodative effects. The geometry of the *ultimate* product would seem kinetically counter-intuitive given the clear *trans* influence that is apparent in the molecular structure of **5.** That said, it should be noted that a dissociative pathway would involve a five-coordinate intermediate, the lifetime of which may well be sufficient as to allow *pseudo*-rotation to reposition the vacant site *cis* to the boron, *i.e.,* the final stereochemistry adopted need not necessarily reflect the site of initial dissociation. This is in contrast to substitution reactions of **1a** wherein the triptych cage with more constrained geometry is less able to undergo rearrangement. Additional details of the molecular structure of **12** will be discussed collectively with further examples below.

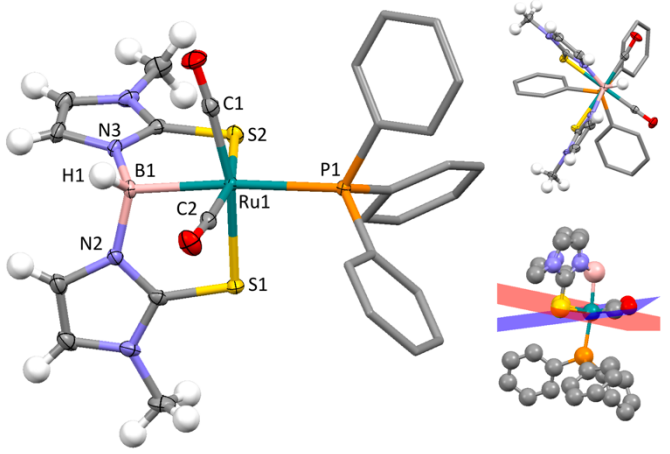

Figure 6. Molecular structure of **12** in a crystal of **12**.$CHCl_3$ (Aryl hydrogen atoms and $CHCl_3$ solvate omitted, phenyl groups simplified, 50% displacement ellipsoids). Selected bond lengths (Å) and angles (°): B1–Ru1 2.237(2), B1–H1 1.03(4), Ru1–P1 2.4740(5), Ru1–C1 1.861(2), Ru1–C2 1.855(2), H1–B1–Ru1 117(2), B1–Ru1–P1 173.72(6), B1–Ru1–C1 82.18(9), B1–Ru1–C2 81.16(9), C1–Ru1–C2 91.77(10). Insets = view along B1–Ru1 vector and representation of angle (18.3°) between the S1–Ru1–S2 (red) and C1–Ru1–C2 (blue) planes.

In contrast to the reversible CO coordination in **1a**, subjecting a crude sample of **12** to vacuum did not result in reformation of **5**. The persistence of complex **12** was instead noted in the ^{1}H and ^{31}P{^{1}H} NMR spectra, which suggested irreversible coordination of the CO ligand. Together these observations suggest that coordination of CO *trans* to the Ru→B linkage is less favourable than coordination *trans* to the π-basic thione donors.

Ligand exchange investigations were extended to consider a range of electronically and sterically variant phosphines. The reaction of **5** with an excess of PMe_3 proceeded cleanly within one hour to give the product of mono-substitution $[Ru(CO)(PMe_3)(PPh_3)\{BH(mt)_2\}]$, the nature of which was inferred from NMR spectroscopic data. The ^{31}P{^{1}H} NMR spectrum revealed the shift to higher frequency of both phosphine resonances relative to **5**, where the broad peak at δ_P = –29.6 suggests the triphenylphosphine ligand was located *trans* to the boron, with the doublet at δ_P = 58.7 ($^2J_{PP}$ = 11.3 Hz) corresponding to coordinated PMe_3. Integration of the ^{31}P{^{1}H} NMR resonances confirmed the liberation of one triphenylphosphine. The inferred product $[Ru(CO)(PMe_3)(PPh_3)\{BH(mt)_2\}]$, however, eluded isolation, despite the promisingly clean NMR spectra acquired for the crude reaction mixture. Failure to isolate the product might reflect the lability and/or volatility of PMe_3. Therefore, investigations were followed up with the less volatile PMe_2Ph, which has electronic and steric properties not dissimilar to PMe_3. As with the reactivity observed with PMe_3, complex **5** was found to react with an excess of PMe_2Ph at room temperature to afford a single substitution product, $[Ru(CO)(PMe_2Ph)(PPh_3)\{BH(mt)_2\}]$ **13** (Scheme 5).

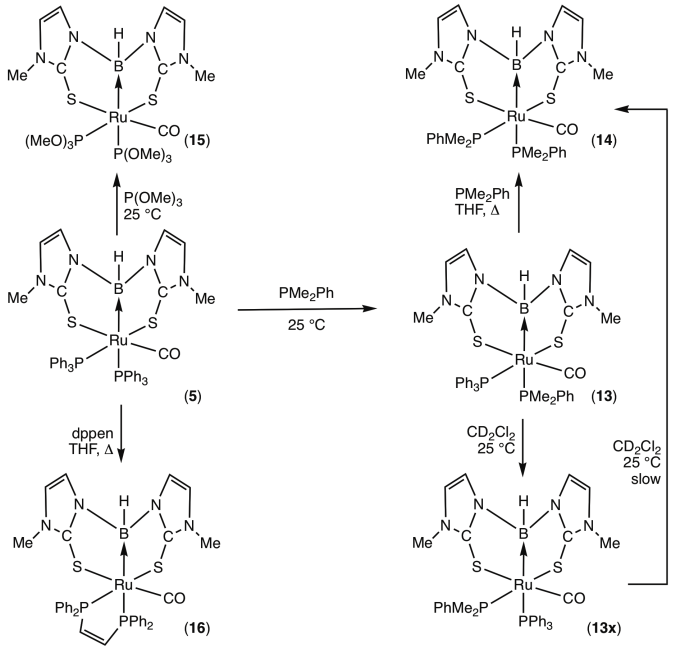

Scheme 5. Phosphine substitution reactions of **5**.

Interestingly, substitution of the second phosphine was not observed spectroscopically under these mild reaction conditions, despite the presence of excess PMe_2Ph. The spectroscopic data resemble those observed for the complex $[Ru(CO)(PMe_3)(PPh_3)\{BH(mt)_2\}]$. The broad resonance at δ_P = –17.2 was attributed to the PMe_2Ph ligand coordinated *trans* to the Ru→B bond, while the relatively sharp doublet at δ_P = 56.9 ($^1J_{PC}$ = 11.3 Hz) was assigned to the larger PPh_3 ligand coordinated *trans* to one thione. The use of PMe_2Ph over the more symmetrical PMe_3 is advantageous in that the two methyl groups provide an indication of the local symmetry of the complex. The asymmetric (C_1) nature of **13** was thus evident from ^{1}H NMR spectroscopy with the diastereotopic methyl groups of PMe_2Ph manifested as chemically inequivalent doublets at δ_H = 1.43 ($^1J_{HP}$ = 5.3) and 1.28 ($^1J_{HP}$ = 5.5 Hz); whilst the remaining ^{1}H signals show similarity to those of **5**. Although crystals of **13** suitable for X-ray diffraction studies were not obtained, the formulation of **13** was supported by the identification of the $[M + H]^+$ peak at *m/z* = 769.1099 in the ESI-MS.

The overnight acquisition of the $^{13}C\{^1H\}$ NMR spectrum of a pure sample of **13** revealed several (≈6) resonances in the region typical of N-methyl mt substituents (δ_C = 33.5–34.2). These appeared as distinct resonances in the ^1H NMR spectrum (measured after ^{13}C data acquisition, See ESI Figure S1) at δ_H = 3.44 and 3.48 (minor) and at δ_H = 3.30 and 3.35 (major). The decomposition of **13** into these products occurred over 10 minutes from dissolution in $CDCl_3$, reaching equilibrium at room temperature to provide a relative ratio of 2:3:5 for **13**, the minor product, and the major product. The formation of these products was initially suspected to be due to the residual acidity of the $CDCl_3$ solvent. However, similar patterns emerged when the less acidic CD_2Cl_2 was used as the solvent.

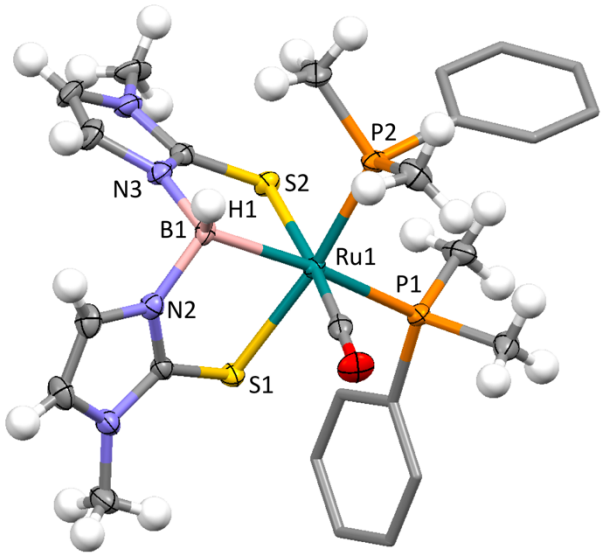

Figure 7. Molecular structure of **14** in a crystal of **14** (Phenyl hydrogen atoms omitted, phenyl groups simplified, 50% displacement ellipsoids). Selected bond lengths (Å) and angles (°): B1–Ru1 2.253(4), B1–H1 1.09(6), Ru1–P1 2.4095(9), Ru1–P2 2.2876(9), Ru1–C1 1.821(4), H1–B1–Ru1 120(3), B1–Ru1–P1 171.51(11), B1–Ru1–P2 88.00(11), B1–Ru1–C1 88.78(16), P1–Ru1–P2 99.57(3)..

To encourage conversion of **13** to the products previously observed in $CDCl_3$, an aliquot of the crude reaction mixture of **13** in THF was briefly (≈ 2 minutes) heated to reflux. The NMR spectra showed the clean partial conversion of **13** to complex $[Ru(CO)(PMe_2Ph)_2\{BH(mt)_2\}]$ (**14**), with no evidence for the other decomposition product or the C_s-symmetric isomer of **14**, which remains unknown. Full conversion of **13** to **14** was achieved on a preparative scale by heating in refluxing THF for 18 hours (Scheme 5, Figure 7). The formation of **14** was accompanied by an increased complexity of the methyl region (δ_H = 1.27–1.48, due to the presence of two chemically inequivalent PMe_2Ph ligands, each with a pair of diastereotopic P-CH_3 substituents with associated resonances each being doublets, (two doublets would be expected for the C_s isomer of **14**). Four distinct P-CH_3 resonances were also present in the $^{13}C\{^1H\}$ NMR spectrum of **14**. Two of the PMe_2Ph methyl groups couple to the chemically inequivalent phosphines in a doublet of doublet multiplicity (δ_C = 15.6, $^1J_{CP}$ = 31.2, $^3J_{CP}$ = 3.3; 18.6, $^1J_{CP}$ = 32.3, $^3J_{CP}$ = 4.2 Hz), while the other two P-CH_3 resonances appear only as doublets (δ_C = 16.3, $^1J_{CP}$ = 13.6; 19.4, $^1J_{CP}$ = 16.2 Hz), presumably reflecting a Karplus-type C–P–Ru–P dihedral angular dependence.[32] Although rotation about the Ru–P bond in solution is expected, the steric properties of the phenyl moiety may well dictate conformational preferences. Coordination of two PMe_2Ph ligands was further ascertained by the respective sharp doublet and broad singlet phosphine environments at δ_P = 14.5 ($^2J_{PP}$ = 12.3) and –16.4, respectively, in the $^{31}P\{^1H\}$ NMR spectrum.

By a process of elimination in the ^1H and $^{31}P\{^1H\}$ NMR spectra of resonances corresponding to **13** and **14**, the third product formed from the ambient temperature decomposition of **13** in $CDCl_3$ is suggested to be the isomerised complex **13x** (Scheme 5). The methyl resonances in Figure ESI-S1 consist of two distinct doublets for the PMe_2Ph ligand (δ_H = 1.23, 1.45, $^2J_{HP}$ = 8.5 Hz), whereas the downfield resonances (δ_H = 3.19, 3.24) correspond to the chemically inequivalent *N*-methyl groups of the $HB(mt)_2$ backbone coordinated to a C_1 symmetric centre. The olefinic signals of all three products reside in a similar chemical shift range of 6.40–6.58 ppm, which occluded the identification of the resonances attributable to **13x**. The two dominant resonances in the $^{31}P\{^1H\}$ NMR spectrum further support the assignment of **13x**. Consistent with the other ruthenaboratranes discussed herein, the two phosphine associated resonances resolve as a broadened signal at δ_P = 22.0 and a sharp doublet at δ_P = 12.9 ($^2J_{PP}$ = 11.4 Hz), which were assigned to PPh_3 and PMe_2Ph, respectively.

Compared to PMe_3 and PMe_2Ph, trimethylphosphite has a smaller steric profile and greater π-acidity. Treatment of **5** with a three-fold excess of $P(OMe)_3$ for 18 hours at room temperature yielded the product of double substitution, the complex $[Ru(CO)\{P(OMe)_3\}_2\{BH(mt)_2\}]$ **15**. Whilst the crude $^{31}P\{^1H\}$ NMR spectrum revealed several (≈10) resonances, complex **15** was evident as the dominant species and could be purified through recrystallisation from diethyl ether and n-pentane. The formulation of **15** was established by NMR spectroscopy, mass spectrometry and a single crystal X-ray diffraction study (Figure 8).

In addition to the characteristic resonances resulting from the $\{BH(mt)_2\}$ moiety in the ^1H NMR spectrum, doublets at δ_H = 3.67 ($^3J_{HP}$ = 11.1 Hz) and 3.56 ($^3J_{HP}$ = 10.8 Hz), are consistent with the coordination of two chemically inequivalent $P(OMe)_3$ ligands. Given the electronegatively inductive (*I*⁻) effects of the methoxy substituents, the two $P(OMe)_3$ resonances were observed as a doublet at δ_P = 151.1 ($^2J_{PP}$ = 19.4 Hz) and a broad singlet at δ_P = 153.7, both as expected, downfield compared to complexes **5** and **12**-**14** of this series. The replacement of both triphenylphosphine ligands in **5** by $P(OMe)_3$ was further demonstrated in the $^{13}C\{^1H\}$ NMR spectrum by an absence of signals in the aromatic region and the appearance of two resonances in the methoxy region (δ_C = 50.8, 52.0). The effect of the quadrupolar boron nuclei appears to extend to the methyl carbon resonance of the $P(OMe)_3$ ligand to which it is *trans* coordinated, which results in broadening for the former resonance. Meanwhile, the latter resonance for the equatorial phosphite ligand remains unaffected, appearing as a sharp doublet ($^2J_{PP}$ = 5.9 Hz).

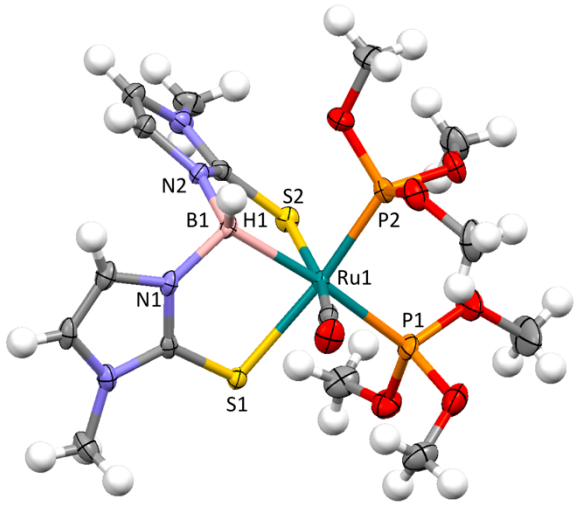

Figure 8. Molecular structure of **15** in a crystal (50% displacement ellipsoids, one of three crystallographically distinct molecules shown). Selected bond lengths (Å) and angles (°): B1–Ru1 2.252(3), B1–H1 1.17(5), Ru1–P1 2.3604(8), Ru1–P2 2.2341(8), Ru1–C1 1.835(3), H1–B1–Ru1 122(3), B1–Ru1–P1 173.33(9), B1–Ru1–P2 86.67(9), B1–Ru1–C1 81.66(13), P1–Ru1–P2 99.56(3).

A notable difference in the reactivity of **5** with PMe_2Ph or PMe_3 compared to $P(OMe)_3$ is the ease of the second PPh_3 substitution. Single substitution predominately occurs with the electron rich alkyl phosphines at room temperature, and introduction of the second equivalent can be achieved only at elevated temperatures. In contrast, substitution with $P(OMe)_3$ occurs readily at room temperature with replacement of both triphenylphosphines. This is most likely a corollary of the greater capacity of π-acidic $P(OMe)_3$ to stabilize the electron rich Ru(0) centre *cf.* PPh_3. This is reflected by the IR shift to higher frequency from 1908 cm^{-1} in **5** to 1921 cm^{-1} in **15**. Furthermore, replacement of the bulky PPh_3 with $P(OMe)_3$ is sterically favourable (θ_T° 145 *cf.* 107°, respectively).

Previous investigations on triptych ruthenaboratranes[8] derived from **1a** revealed that $[Ru(CO)(PCy_3)\{B(mt)_3\}]$ could not be isolated from the reaction of **1a** with PCy_3 because an equilibrium between PPh_3 and PCy_3 coordination developed. An alternative approach utilised the complex $[RuCl(Ph)(CO)(PCy_3)_2]$ in a direct reaction with $Na[HB(mt)_3]$ which obviated the competitive presence of PPh_3. Similar synthetic strategies were explored toward the complexes $[Ru\{BH(mt)_2\}(CO)(PCy_3)(PPh_3)]$ and $[Ru\{BH(mt)_2\}(CO)(PCy_3)_2]$ without success. It should be noted that whilst the sterically congested *cis*-$Ru(PCy_3)_2$ fragment is understandably rare, it is not unknown.[33] The room temperature reaction of **5** with two equivalents of PCy_3 in THF for 20 hours yielded mainly starting material and numerous minor products (~10 resonances in the $^{31}P\{^1H\}$ NMR spectrum). Heating under reflux for four hours facilitated further development of these resonances with the concurrent appearance of free PPh_3 and absence of the starting material. However, the anticipated complex $[Ru\{BH(mt)_2\}(CO)(PCy_3)(PPh_3)]$ and other products could not be conclusively identified. Further attempts with a stoichiometric amount of PCy_3 at room temperature and at reflux, in Et_2O and THF, showed either no reaction or produced ^1H and $^{31}P\{^1H\}$ NMR spectra that were similarly abundant in unidentifiable resonances. No dynamic phosphine exchange was inferred from the sharp resonance for the liberated PPh_3.

To eliminate possible complication of mixed PPh_3/PCy_3 coordination, the synthesis of the PCy_3 analogue of **5** was pursued through reaction of $Na[H_2B(mt)_2]$ with $[RuPhCl(CO)(PCy_3)_2]$ in THF. The solution IR spectrum in THF of the crude reaction mixture displays a CO band of low stretching frequency 1898 cm^{-1}, amongst others (ν_{CO} = 1918, 1988 cm^{-1}). This is indicative of ruthenium in the zero-oxidation state and falls within the range 1877–1921 cm^{-1} established for the ruthenaboratranes synthesised thus far and whilst these IR data were promising, the presence of four *sharp* resonances of equal intensity in the $^{31}P\{^1H\}$ NMR spectrum suggested the absence of phosphine coordination *trans* to the boron. Despite numerous crystallisation experiments, only amorphous powder unsuitable for X-ray diffraction studies was obtained. The complications associated with the introduction of PCy_3 may be sterically and/or electronically disfavoured *cf.* PPh_3. The steric bulk of the PCy_3 ligand is considerably greater than that of PPh_3, and therefore it may be unfavourable to adjacently accommodate two of these ligands around the ruthenium centre. From the substitution reactions investigated thus far, the substitution process appears to be most facile and favoured for π-acidic ligands, such that the σ-basicity of the PCy_3 ligand may disfavour its coordination to the electron rich Ru(0) centre.

The replacement of both PPh_3 ligands in **5** in the synthesis of complexes **14** and **15** led to the natural extension of the substitution reactivity to the inclusion of bidentate ligands. Given the *cis* arrangement of the PPh_3 ligands in **5**, *Z*-1,2-bis(diphenylphosphino)ethylene (dppen), was envisaged as a suitable bidentate ligand to ensure chelation, rather than formation of bridged binuclear species as might be anticipated for the more commonly employed 1,2-bis(diphenylphosphino)ethane (dppe) ligand. The conversion of **5** to $[Ru\{BH(mt)_2\}(CO)(Ph_2PCH{=}CHPPh_2)]$ **16** took place in THF under reflux for 43 hours, evident by the development of two downfield resonances at δ_P = 70.6 (d, $^2J_{PP}$ = 8.1) and 50.8 (broad) in the $^{31}P\{^1H\}$ NMR spectra. The vinylic hydrogen resonances of the phosphine were obscured within the aromatic region but could be located from $^1H^{13}C$ HSQC experiments as multiplets at δ_H = 7.91 and 7.97. The corresponding $^{13}C\{^1H\}$ shifts appear as two doublet of doublet resonances, respectively at δ_C = 148.1 ($^1J_{CP}$ = 26.6, $^2J_{CP}$ = 26.6) and 149.0 ($^1J_{CP}$ = 35.8, $^2J_{CP}$ = 45.5). The C_1 symmetry of **16** and the rigidity of the ethylene backbone renders each phenyl on the dppen chelate inequivalent. The molecular structure of **16** was confirmed by an X-ray diffraction study, as depicted in Figure 9 and discussed below.

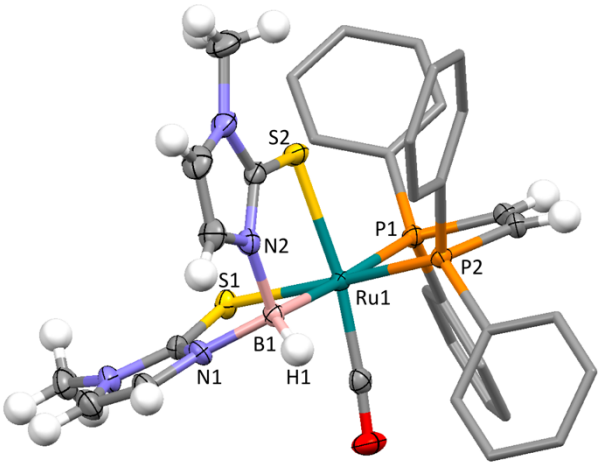

Figure 9. Molecular structure of **16** (aryl hydrogen atoms omitted, phenyl groups simplified, displacement ellipsoids shown at 50%). Selected bond lengths (Å) and angles (°): B1–Ru1 2.231(2), B1–H1 1.09(4), Ru1–P1 2.3636(5), Ru1–P2 2.2719(5), Ru1–C1 1.848(2), H1–B1–Ru1 121(2), B1–Ru1–P1 175.39(6), B1–Ru1–P2 91.81(6), B1–Ru1–C1 86.26(9), P1–Ru1–P2 85.29(2)

The triptych ruthenaboratrane **1a** undergoes clean and irreversible substitution of the PPh_3 ligand by isonitriles CNR (R = ^{t}Bu, $C_6H_2Me_3$-2,4,6, $C_6H_3Me_2$-2,6).[1b] Whilst **5** reacts readily with CN^{t}Bu and $CNC_6H_2Me_3$-2,4,6 at room temperature, liberating free PPh_3, difficulties in purification precluded the isolation of the desired products, [Ru{BH(mt)$_2$}(CO)(PPh_3)(CNR)] (R = ^{t}Bu, $C_6H_2Me_3$-2,4,6). The infrared spectrum measured within two hours of the reaction between **5** and CN^{t}Bu in THF contained numerous overlapping peaks at 2109–2200 cm^{-1}, as well as free CN^{t}Bu (2070 cm^{-1}). The dominant bands at ν_{CN} = 2134 and ν_{CO} = 1924 cm^{-1} may be evidence of the product of mono-substitution, [Ru{BH(mt)$_2$}(CO)(PPh_3)(CN^{t}Bu)]. Although a stoichiometric amount of $CNC_6H_2Me_3$-2,4,6 was used in reaction with **5**, incomplete reactivity was inferred by the presence of free $CNC_6H_2Me_3$-2,4,6 (ν_{CN} = 2112 cm^{-1}) in the IR spectrum after an extended period (43 hours). Despite the plethora of resonances (~11) in the $^{31}P\{^1H\}$ NMR spectrum, the IR spectrum following recrystallisation from THF/n-pentane showed evidence of the postulated product [Ru{BH(mt)$_2$}(CO)(PPh_3)(CNMes)] with stretching frequencies of ν_{BH} = 2360, ν_{CN} = 2088, and ν_{CO} = 1919 cm^{-1}, in a mixture with an unidentified carbonyl containing complex at ν_{CO} = 1954 cm^{-1}, a value inconsistent with zerovalent ruthenium. Neither fractional crystallisation nor column chromatography resulted in the isolation of a single pure material.

Treatment of **5** with HC_5Me_6 (HCp*) was envisaged as a potential alternative route to Goh's borate complex [Cp*Ru(CO){κ^2-*S,S'*-H_2B(mt)$_2$}],[19h] which is akin to [Cp*Ru(CO){κ^2-*S,S'*-H_2B(azain)$_2$}] (azain = 7-azaindolyl),[34] thereby concomitantly probing phosphine substitution and Ru→B reactivity. No reaction occurred at room temperature, while raising the temperature to 80°C resulted in a mixture of products. These results perhaps unsurprisingly parallel those for HC≡CPh and $HBO_2C_6H_4$ discussed above in that the thermal conditions required for the Ru→B bond to participate directly in reactions appear incompatible with the endurance of the resulting products. This contrasts with the facile insertion of CS into a Rh→B bond leading to the unusual thioketone complex [RhH(PPh_3){η^2-*C,S*:κ^2-*S',S''*-SC(PPh_3)BH(mt)$_2$}].[14] Treating **5** with CS_2 might have been expected to afford the thiocarbonyl containing ruthenaboratrane [Ru(CS)(CO)(PPh3){BH(mt)$_2$}], akin to [Ru(CS)(PPh_3){B(mt)$_3$}],[1b] however no reaction was observed at room temperature, despite the phosphine lability demonstrated above and the irreversible coordination of CS_2 to other zerovalent ruthenium centres established elsewhere.[35] At higher temperatures decomposition ensued with cleavage of the borane ligand and formation of free methimazole.

Analysis and Comparison of Data

The series of complexes of the form [Ru(CO)(L^1)(L^2){BH(mt)$_2$}] synthesised from phosphine substitution reactions of **5** allow an appraisal of the effect of various co-ligands on the Ru→B bond, in addition to a comparison with the triptych derivatives, [Ru(CO)(L){B(mt)$_3$}].[1,8] The key structural features of complexes [Ru(CO)(L^1)(L^2){BH(mt)$_2$}] (**5**, **12**, **14**, **15** and **16**) and [Ru(CO)(PPh_3){B(mt)$_3$}] (**1a**) are summarised in Table 1.

Table 1. Selected Geometric and Spectroscopic Data for Diptych Ruthenaboratranes [Ru(CO)(L^1)(L^2){BH(mt)$_2$}] (L^2 *trans* to Boron)

L^1	L^2	Ru→B [Å]	Ru–P(L^1) [Å]	Ru–P(L^2) [Å]	δ_B [ppm]	ν_{CO} [cm^{-1}]
PMe_2Ph	PMe_2Ph	2.253(4)	2.288(1)	2.4094(8)	5.00	1877
PMe_2Ph	PPh_3	-	-	-	5.13	1890
PPh_3	PPh_3	2.246(2)	2.3044(4)	2.4766(4)	4.12	1893
$Ph_2PCH{=}CHPPh_2$		2.231(1)	2.2720(5)	2.3637(6)	5.05	1905
$P(OMe)_3$	$P(OMe)_3$	2.252(3)	2.2340(9)	2.3604(9)	3.80	1921
CO	PPh_3	2.237(2)	–	2.4741(5)	2.97	1913, 1984
mt[a]	*PPh_3*	*2.161(7)*	-	*2.435(1)*	*17.1*	*1988*

[a] [Ru(CO)(PPh_3){B(mt)$_3$}].[1,8]

The [Ru(CO)(L^1)(L^2){BH(mt)$_2$}] series is ordered in Table 1 by increasing CO stretching frequency. This trend represents the relative decrease of electron density (π-basicity) of the ruthenium centres and parallels the progressive change of electronic properties of the phosphine ligands from σ-basic PMe_2Ph to π-acidic $P(OMe)_3$. For the triptych analogues (ν_{CO} = 1871 –1894 cm^{-1}),[8] this was shown to correlate well with Tolman's [Ni(CO)$_3$(L)]-derived electronic parameter[36] and a similar trend is reproduced here and consistent with this observation, the ν_{CO} stretching frequency of **14** is some 44 cm^{-1} lower than **15**. Whilst retrodonation to carbonyl ligands involves metal orbitals of π-symmetry with respect to the M-L axes ('t_{2g} type'), retrodonation to boron involves a metal orbital of σ-symmetry ('e_g type') such that variations in one will only indirectly perturb the other. There is no absolute correlation between Tolman's electronic parameter and the Ru→B bond length, e.g., the two extremes of the series **14** (L^1 = L^2 = PMe_2Ph) and **15** (L^1 = L^2 = $P(OMe)_3$) have crystallographcally identical Ru-B bond lengths (2.253(4) and 2.252(3) Å, respectively). It should also be noted that the Tolman cone angles for these two comparatively compact ligands are not so dissimilar (122 *cf.* 107°). The shortest Ru→B bond length is observed for the dppen derivative **16** (2.231(1)Å) however that is perhaps to be expected given that the dppen chelate subtends an acute bite angle (85.29(2)°) whilst in all other cases the L^1-Ru-L^2 angle

between donor atoms is obtuse. It must be stressed that for this series of similar complexes, the range of Ru→B bond lengths spans only some 22 pm whilst the precision for comparison of bond lengths (6 x e.s.d.) spans 6 – 24 pm, due in part to the caveats associated with locating comparatively light atoms such as boron, adjacent to heavy metal atoms, i.e., this geometric parameter is not likely to be reliably informative. Indirect insights into the impact of Ru→B bonding are, however, provided by the more precisely determined Ru–P bond lengths. In every case where two phosphines are present, the Ru–P bond length *trans* to the Ru→B bond is very significantly longer than that *trans* to the thione, by as much as 0.058 Å in the case of **5**. However, it should be noted that whilst **5** has the greatest disparity, this should not be attributed to the Ru-B *trans* influence alone, since of all the phosphines employed, PPh_3 has the largest Tolman cone angle, *i.e.*, there will be a steric as well as electronic component operating. The difference in bond lengths was found to be least pronounced for complex **16** with the bidentate dppen ligand, which may reflect the constraints of chelation over electronic considerations. Notably, no viable correlation could be inferred between the elongated Ru–L_2 bond and the Ru→B bond distance.

Tricoordinate boranes are typically planar ($\Sigma°BX_3 \approx 360°$), with pyramidalisation of the boron attending interaction with a metal (M→BX_3; ideal tetrahedron ($\Sigma°BX_3 \approx 328°$). Thus, the degree of pyramidalisation at the boron environment might be used to estimate the strength of the Ru→B bond.[7c,37] Notwithstanding the usual caveats associated with the precision of hydrogen atom positions in X-ray analysis, the angle sum $\Sigma°BX_3$ values of the complexes in the [Ru(CO)(L^1)(L^2){BH(mt)$_2$}] series span a comparatively narrow range of 317.5–326.1° bounded by **5** and **12** (Figure 10).

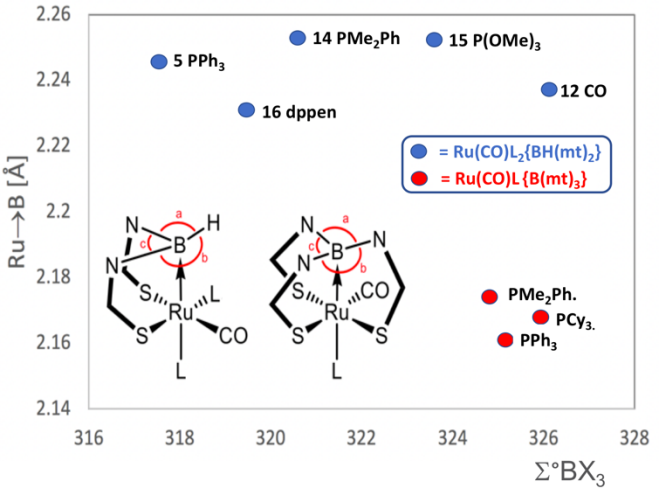

Figure 10. Lack of relationship between the Ru→B distance and the pyramidalization sum around the boron ($\Sigma°BX_3$) for complexes [Ru(CO)L_2{BH(mt)$_2$}] (blue) and [Ru(CO)L{B(mt)$_3$}][8] (red) .

A narrower range of 324.9–325.9° was established by the [Ru{B(mt)$_3$}CO(L)] series. The geometry around boron deviates far from planarity in both series. This suggests a stronger M→B interaction than in Bourissou's Group 9, 10 and 11 metallaboratranes based on ambiphilic di- or tri- phosphino borane ligands adopting larger (*i.e.*, more trigonal) $\Sigma°BX_3$ values (e.g., Group 10, M→B: 341.8–336.7).[7c,36] The variation of pyramidalisation is most remarkable between **5** and **12** where the smaller $\Sigma°BX_3$ value (greater pyramidalisation) of the former may result from the greater steric imposition of PPh_3 on the boron environment than CO. Indeed, whilst there is no obvious correlation between the degree of pyramidalization and associated Ru→B bond length (Figure 10), there is a monotonic relationship between pyramidalization and the Tolman steric parameter (θ_T, Figure 11), notwithstanding the uncertainties of defining such a parameter for CO (95°)[36] and for chelating dppen, which we have approximated to $PMePh_2$. This somewhat over-estimates the steric profile of each half of the dppen ligand given the constraints of chelation and the associated preclusion of free rotation around the metal-phosphorus bond, an assumption upon which the Tolman parameter is based. Thus there is most likely even better correlation than might be suggested by the approximation to $PMePh_2$. Thus deformation of the boron coordination sphere, appears to be a plausible response to steric congestion that need not significantly compromise Ru→B binding.

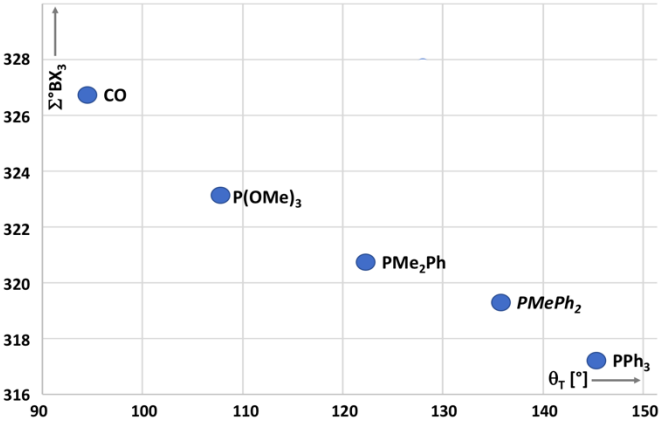

Figure 11. Correlation between the pyramidalization at boron and the Tolman steric parameter,[35] θ_T, for the complexes [Ru(CO)L_2{BH(mt)$_2$}].

Conclusions

The syntheses of diptych ruthenaboratranes have been developed, with the first example [Ru(CO)(PPh_3)$_2${BH(mt)$_2$}] (**5**) providing access to further examples via mono or disubstitution of the PPh_3 ligands. Whilst extensive structural data attest to a significant *trans influence* on the part of the Ru→B bond, the *trans effect* is somewhat more subtle in that the kinetic products of monosubstitution (**12**,**13**) have the extraneous ligand positioned *cis* to the Ru→B bond. We attribute this to the geometric flexibility of the 5-coordinate intermediate arising from initial PPh_3 dissociation, with rearrangement to present the vacant coordination site in the *cis* position rather than *trans* to the Ru→B bond. Implicit in this interpretation is the reluctance of CO to assume the position *trans* to the Ru-B bond rather than the more σ-basic phosphorus ligands, which would also tally with the lability of the CO ligand observed in the triptych system for [Ru(CO)$_2${B(mt)$_3$}].[1b] We are unable at this stage to discount arrival at the thermodynamic isomer via an initially formed kinetic isomer that undergoes a subsequent

non-dissociative isomerism such as the Ray-Dutt or Bailar twist mechanisms.[38] We have previously observed such a process to occur upon heating octahedral cationic triptych rhodaboratranes[22] and Ball and Mann have provided NMR-derived evidence for $[RuH_2(CO)(PPh_3)_3]$ undergoing intramolecular phosphine site exchange upon heating.[37d] Given the mild conditions employed herein, we remain disposed towards the 5-coordinate pseudo-rotation interpretation. It should however be noted in this context that 5-coordinate rhodaboratranes have been isolated in which the ground state has the contrary geometry with a vacant site *trans* to the Rh→B bond, *e.g.*, Bourissou's 2-phosphinoaryl borane archetype $[RhCl(DMAP)\{BPh(C_6H_4P^iPr_2\text{-}2)_2\}]$,[7a] the preference for reduced coordination numbers for group 9 (*cf.* group 8) notwithstanding.

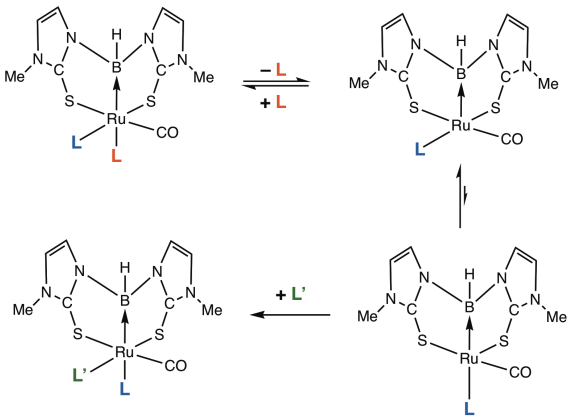

Scheme 6. Regioselectivity of ligand substitution in diptych ruthenaboratranes.

The peculiarities of the coordination chemistry of *Z*-type (*i.e.*, σ-Lewis acidic) ligands[39] in contrast to more classical electron-pair donor ligands (X, L) would seem to call for further study.

Experimental

General Consideration - All manipulations were carried out under a dry and oxygen-free nitrogen atmosphere using standard Schlenk vacuum line, and inert atmosphere dry-box techniques, with dried and degassed solvents that were distilled from either calcium hydride (CH_2Cl_2) or sodium and benzophenone (ethers, hexane, THF, toluene, xylene and paraffins). NMR spectra were obtained at 298 K on a Varian Mercury 300 (^{1}H: 300.1 MHz, ^{31}P: 121.5 MHz), a MR 400 (^{1}H: 399.8 MHz, ^{31}P: 161.8 MHz), a Bruker Avance 400 (^{1}H: 400.1 MHz, ^{11}B: 128.4 MHz, ^{13}C: 100.6 MHz, ^{31}P: 162.0 MHz), a Bruker Avance 600 (^{1}H: 600.0 MHz, ^{13}C: 150.9 MHz), or a Bruker Avance 700 (^{1}H: 700.2 MHz, ^{13}C: 176.1 MHz, ^{31}P: 283.5 MHz). ^{1}H chemical shift (δ) data were referenced to residual solvent peaks in deuterated solvent. ^{13}C chemical shift (δ) data were referenced to the resonances of the deuterated solvent. ^{31}P and ^{11}B were referenced to external 85% H_3PO_4 or $BF_3.OEt_2$ standards, respectively. Infrared spectra were obtained with a Bruker Alpha FTIR with diamond plate Attenuated Total Reflectance sampling attachment, run at 4 cm^{-1} resolution. Solution infrared spectra were obtained using a Perkin-Elmer Spectrum One FT-IR Spectrometer. Elemental microanalysis was performed by the London Metropolitan University. Electrospray (ESI) mass spectrometry were performed by the Research School of Chemistry mass spectrometry service. Data for X-ray crystallography were collected with an Agilent SupaNova diffractometer. The complexes $[RuCl(Ph)(CO)(PPh_3)_2]$[15] and $[RuCl(CH{=}CHPh)(CO)(PPh_3)_2]$[16] and the pro-ligand salt $Na[H_2B(mt)_2]$[17] were prepared as described previously. Other reagents were used as received from commercial suppliers.

Synthesis of $[Ru(CO)(PPh_3)_2\{BH(mt)_2\}]$*(Ru→B)*[8] (5). *Method 1:* A suspension of $[RuCl(Ph)(CO)(PPh_3)_2]$ (0.500 g, 0.65 mmol) and $Na[H_2B(mt)_2]$ (0.175, 0.67 mmol) in diethyl ether (50 mL) was stirred for 15 h, by which time the suspension had lightened from an orange colour to beige. The solvent was removed in vacuo and the resulting residue was re-dissolved in dichloromethane (30 mL). The filtrate was transferred to another Schlenk flask by cannula filtration. An equal volume of ethanol was added, and the solvent was removed slowly under reduced pressure to afford a beige precipitate that was filtered and dried under high vacuum. Yield: 0.198 g (0.222 mmol, 34%). *Method 2:* A suspension of $[RuHCl(CO)(PPh_3)_3]$ (1.000 g, 1.05 mmol) and ethynylbenzene (0.30 mL, 2.7 mmol, excess) in dichloromethane (35 mL) was stirred for 1.5 h, by which time the solution had turned to a deep red colour at which point $Na[H_2B(mt)_2]$ (0.275 g, 1.05 mmol) was added. The reaction mixture was stirred for a further 18 h, and the filtrate isolated by cannula filtration. The solvent was concentrated in vacuo to ≈ 5 mL. Diethyl ether (20 mL) was added to the yellow oily residue, to afford a pale yellow solid that was isolated by cannula filtration. Petroleum ether was added and the solid collected on a sintered funnel, washed with diethyl ether and petroleum ether, then dried under high vacuum. Yield: 0.570 g (0.639 mmol, 61%). Crystals of a diethyl ether solvate suitable for crystallographic analysis were obtained from slow evaporation of a concentrated solution of **5** in diethyl ether over one day. IR (ATR, cm^{-1}): 2316 ν_{BH}, 1893 ν_{CO}. IR (CH_2Cl_2): 2397 ν_{BH}, 1899 ν_{CO}. ^{1}H NMR (400 MHz, $CDCl_3$): δ_H = 3.07, 3.33 (s x 2, 3 H x 2, CH_3), 4.07 (s, v.br., 1 H, BH), 6.04 (d, 1 H, $^3J_{HH}$ = 1.8, NCH=CH), 6.15 (d, 1 H, $^3J_{HH}$ = 1.8, NCH=CH), 6.50 (d, ^{1}H, $^3J_{HH}$ = 1.7, NCH=CH), 6.58 (d, 1 H, $^3J_{HH}$ = 1.8, NCH=CH), 6.97 – 7.07 (m, 9 H, C_6H_5), 7.22 – 7.26 (m, 9 H, C_6H_5), 7.40 – 7.47 (m, 12 H, C_6H_5). ^{13}C{^{1}H} NMR (176 MHz, $CDCl_3$): δ_C = 33.7, 34.1 (CH_3 x 2), 119.8 (NCH=CH), 120.3 (NCH=CH), 120.7 (NCH=CH), 120.9 (NCH=CH), 126.4 [d, $^{2,3}J_{CP}$ = 8.8, $C^{2,3,5,6}(C_6H_5)$], 127.5 [br, $C^{2,3,5,6}(C_6H_5)$ for PPh_3 *trans* to B), 128.1 [d, $^4J_{CP}$ = 1.8, $C^4(C_6H_5)$], 128.5 [C4(C_6H_5) for PPh_3 *trans* to B), 134.3 [d, $^{2,3}J_{CP}$ = 14.1, $C^{2,3,5,6}(C_6H_5)$ for PPh_3 *trans* to B), 134.5 (d, $^{2,3}J_{CP}$ = 8.8, $C^{2,3,5,6}(C_6H_5)$], 137.1 [d, $^1J_{CP}$ = 19.4, $C^1(C_6H_5)$ for PPh_3 *trans* to B), 137.9 [d, $^1J_{CP}$ = 40.5, $C^1(C_6H_5)$], 163.6, 164.8 (CS x 2), 208.5 (d, $^2J_{CP}$ = 15.6, CO). ^{31}P{^{1}H} NMR (162 MHz, $CDCl_3$): δ_P = 52.7 (s.br., PPh_3 *trans* to S), 19.3 (s.br., PPh_3 *trans* to B, $^2J_{PP}$ not resolved). ^{11}B{^{1}H} NMR (128 MHz, $CDCl_3$): δ_B = 4.12 (s.br.). ^{11}B NMR (128 MHz, $CDCl_3$): δ_B = 3.81 (s.br., $^1J_{BH}$ not resolved). ESI-MS(+) *m/z* = 895.2 $[M–CO+OMe]^+$. Accurate mass: Found 895.1592 $[M–CO+OMe]^+$, Calcd. for $C_{45}H_{44}{}^{11}BN_4OP_2{}^{102}RuS_2$: 895.1568. Anal. Found: C, 60.52; H, 4.77; N, 6.13%. Calcd. for $C_{45}H_{41}BN_4OP_2RuS_2$: C, 60.61; H, 4.63; N, 6.28%. *Crystal data for* $C_{45}H_{41}BN_4OP_2RuS_2.C_4H_{10}O$ at 185 K: M_w = 965.93, monoclinic,

$P2_1/n$, a = 12.2007(3) Å, b = 24.2676(5) Å, c = 15.8232(3) Å, β = 99.4773(19) °, V = 4621.02(9) Å^3, Z = 4, D_{calcd} = 1.388 Mg m^{-3}, μ(Mo Kα) = 0.54 mm^{-1}, T = 185(2) K, clear pale yellow block, 0.14 x 0.10 x 0.06 mm, 10,695 independent reflections. F^2 refinement, R_1 = 0.037, wR_2 = 0.070 for 8,455 reflections (I > 2.0σ(I), $2\theta_{max}$ = 60°), 553 parameters, 0 restraints. *Crystal data for* $C_{45}H_{41}BN_4OP_2RuS_2.C_4H_{10}O$: M_w = 965.93, monoclinic, $P2_1/n$, a = 12.2141(1) Å, b = 24.2890(2) Å, c = 15.8351(1) Å, β = 99.4996(7)°, V = 4633.35 (3) Å^3, Z = 4, D_{calcd} = 1.385 Mg m^{-3}, μ(Cu Kα) = 4.57 mm^{-1}, T = 150(2) K, clear pale yellow block, 0.12 x 0.08 x 0.08 mm, 9,370 independent reflections. F^2 refinement, R_1 = 0.023, wR_2 = 0.058 for 9,370 reflections (I > 2.0σ(I), $2\theta_{max}$ = 144°), 553 parameters, 0 restraints CCDC1881115. *Crystal data for* [Ru(Ph)(κ^2-*N,S*-mt)(CO)(PPh_3)$_2$] (**6**), see also Reference 21. $C_{47}H_{40}N_2OP_2RuS$: M_w = 843.93, monoclinic, $P2_1/n$, a = 13.1748(1) Å, b = 18.1695(1) Å, c = 17.5732(1) Å, β = 110.7668(8)°, V = 3933.36(2) Å^3, Z = 4, D_{calcd} = 1.425 Mg m^{-3}, μ(Cu Kα) = 4.79 mm^{-1}, T = 150(2) K, clear light yellow needle, 0.22 x 0.05 x 0.04 mm, 7,972 independent reflections. F^2 refinement, R_1 = 0.024, wR_2 = 0.062 for 7,260 reflections (I > 2.0σ(I), $2\theta_{max}$ = 60°), 487 parameters, 0 restraints. *Crystal data for* [Ru(C≡CPh)(CO)(PPh_3){H_2B(mt)$_2$}] (**8**) $C_{35}H_{32}BN_4OPRuS_2$-$CHCl_3$: M_w = 850.98, triclinic, P-1 (No. 2), a = 9.9810(7) Å, b = 11.0018(6) Å, c = 19.3279(8) Å, α = 73.725(4)°, β = 82.147(4)°, γ = 65.670(6)°, V = 1855.8(2) Å^3, Z = 2, D_{calcd} = 1.523 Mg m^{-3}, μ(Cu Kα) = 7.15 mm^{-1}, T = 150(2) K, yellow prism, 0.11 x 0.08 x 0.04 mm, 7,474 independent reflections. F^2 refinement, R_1 = 0.032, wR_2 = 0.083 for 6,775 reflections (I > 2.0σ(I), $2\theta_{max}$ = 144°), 450 parameters, 0 restraints, CCDC 1881116.

Reaction of [Ru(CO)(PPh_3)$_2${BH(mt)$_2$}] with HCl. An ethereal solution of hydrogen chloride (0.25 mL, 1M, 0.25 mmol) was added to a stirred solution of [Ru(CO)(PPh_3)$_2${BH(mt)$_2$}] (**5**: 0.200 g, 0.22 mmol) in tetrahydrofuran and the mixture was stirred for 24 h. The $^{31}P\{^1H\}$ NMR spectrum revealed a mixture of products at δ_P = 55.2, 50.0, 45.2, 35.7, 28.1 and 19.1 in addition to free triphenylphosphine. The solvent was removed using a rotary evaporator and the orange residue was crystallized from chloroform and n-pentane. The crystals were collected on a sintered frit and dried in air to give a mixture of the products below. Combined yield: 0.073 g.

Product 1: [$RuCl_2$(CO)(PPh_3)$_2$(Hmt)] (**9**): ESI-MS(+) m/z: 803.1 [M–Cl]$^+$, 844.1 [M–Cl + MeCN]$^+$. Accurate mass: Found 803.0754 [M–Cl]$^+$, Calcd. for $C_{41}H_{36}N_2O^{35}Cl_2P_2S^{102}Ru$: 803.0750; Found 844.1021 [M–Cl+MeCN]$^+$, Calcd. for $C_{43}H_{39}N3O^{35}ClP_2S^{102}Ru$: 844.1016. *Crystal data for* $C_{41}H_{36}Cl_2N_2OP_2RuS.CHCl_3$: M_w = 958.11, monoclinic, $P2_1/c$, a = 11.5279(1), b = 20.9802(1), c = 18.3591(2) Å, V = 4222.02(5) Å^3, Z = 4, D_{calcd} = 1.507 Mg m^{-3}, μ(Cu Kα) = 7.38 mm^{-1}, T = 150(2) K, orange needle, 0.18 x 0.05 x 0.05 mm, 8,525 independent reflections. F^2 refinement, R_1 = 0.031, wR_2 = 0.078 for 7,799 reflections (I > 2.0σ(I), $2\theta_{max}$ = 144°), 490 parameters, 0 restraints, CCDC 1881118.

Product 2: [$RuCl_2$(CO)(PPh_3)(Hmt)$_2$] (**10**): Washing the isolated mixture with chloroform and filtering under vacuum suction afforded a second product. IR (ATR, cm^{-1}): 3028 ν_{CH}, 1961 ν_{CO}. ^1H NMR (400 MHz, $CDCl_3$): δ_H = 3.42 (s, 6 H, CH_3), 6.61 (t, 2 H, $^3J_{HH}$ = 2.3, NCH=CH), 6.75 (t, 2 H, $^3J_{HH}$ = 2.4, NCH=CH), 7.30 – 7.33 (m, 9 H, C_6H_5), 7.79 – 7.82 (m, 6 H, C_6H_5), 12.92 (s.br., 2 H, NH). $^{13}C\{^1H\}$ NMR (100 MHz, $CDCl_3$): δ_C = 34.2 (CH3), 115.2 (NCH=CH), 119.5 (NCH=CH), 127.6 [d, $^{2,3}J_{CP}$ = 10.0, $C^{2,3,5,6}(C_6H_5)$], 129.7 [d, $^4J_{CP}$ = 3.0, $C^4(C_6H_5)$], 133.8 [d, $^1J_{CP}$ = 48.3, $C^1(C_6H_5)$], 134.5 [d, $^{2,3}J_{CP}$ = 9.1, $C^{2,3,5,6}(C_6H_5)$], 158.1 (CS). $^{31}P\{^1H\}$ NMR (162 MHz, $CDCl_3$): δ_P = 45.1. ESI-MS(+) m/z: 689.1 [M–H]$^+$, 655.0 [M–Cl]$^+$. Accurate mass: Found 655.0102 [M–Cl]$^+$, Calcd. for $C_{27}H_{27}N_4O^{35}ClPS_2{}^{102}Ru$: 655.0104. *Crystal data for* $C_{27}H_{27}Cl_2N4OPRuS_2$: M_w = 690.58, monoclinic, *Cc*, a = 9.2352(4), b = 16.5996(6), c = 18.7713(7) Å, β = 94.733(4)°, V = 2867.84(19) Å^3, Z = 4, D_{calcd} = 1.599 Mg m^{-3}, μ(Mo Kα) = 0.96 mm^{-1}, T = 150(2) K, yellow block, 0.18 x 0.12 x 0.06 mm, 5,442 independent reflections. F^2 refinement, R_1 = 0.029, wR_2 = 0.065 for 5,212 reflections (I > 2.0σ(I), $2\theta_{max}$ = 144°), 345 parameters, 2 restraints, CCDC 1881117.

Synthesis of [Ru{BH(mt)$_2$}(CO)$_2$(PPh_3)] *(Ru→B)*[8] (12). Carbon monoxide (1 atm) was bubbled through a stirred solution of [Ru(CO)(PPh_3)$_2${BH(mt)$_2$}] (**5**: 0.205 g, 0.23 mmol) in dichloromethane for 15 min. The solvent was removed *in vacuo* to give a yellow residue, which was then suspended in diethyl ether (10 mL). The yellow solid was isolated by cannula filtration, washed with n-pentane (20 mL) and dried under vacuum. Yield: 0.079 g (0.120 mmol, 52%). Crystals of a chloroform solvate **12**.$CHCl_3$ suitable for crystallographic analysis were obtained from slow evaporation of a concentrated solution of **12** in chloroform/n-pentane over one day. IR (ATR, cm^{-1}): 2344 ν_{BH}, 1984, 1913 ν_{CO}. ^1H NMR (700 MHz, $CDCl_3$): δ_H = 3.43 (s, 6 H, CH_3), 6.62 (s, 2 H, NCH=CH), 6.69 (s, 2 H, NCH=CH), 7.36 – 7.39 (m, 9 H, C_6H_5), 7.52 – 7.55 (m, 6H, C_6H_5). $^{13}C\{^1H\}$ NMR (176 MHz, $CDCl_3$): δC = 34.4 (CH_3), 120.9 (NCH=CH), 122.1 (NCH=CH), 128.3 [d, $^{2,3}J_{CP}$ = 8.8, $C^{2,3,5,6}(C_6H_5)$], 129.4 [d, $^4J_{CP}$ = 1.2, $C^4(C_6H_5)$], 133.6 [d, $^{2,3}J_{CP}$ = 13.2, $C^{2,3,5,6}(C_6H_5)$], 136.3 [d, $^1J_{CP}$ = 27.1, $C^1(C_6H_5)$], 163.9 (d, $^3J_{CP}$ = 20.2, CS), 202.9 (d, $^2J_{CP}$ = 2.4, CO). $^{31}P\{^1H\}$ NMR (162 MHz, $CDCl_3$): δ_P = 20.1. ^{11}B NMR (128 MHz, CDCl3): δ_B = 2.97 (s.br.). ESI-MS(+) m/z: 648.1 [M–B]$^+$, 659.0 [M+H]$^+$. Accurate mass: Found 659.0441 [M+H]$^+$, Calcd. for $C_{28}H_{27}{}^{11}BN_4O_2PS_2{}^{102}Ru$: 659.0450. Anal. Found: C, 51.29; H, 3.95; N, 8.37%. Calcd. for $C_{28}H_{26}BN_4O_2PRuS_2$: C, 51.15; H, 3.99; N, 8.52%. *Crystal data for* $C_{28}H_{26}BN_4O_2PRuS_2.CHCl_3$: M_w = 776.90, monoclinic, $P2_1/c$, a = 9.7228(1), b = 18.6012(1), c = 17.8876(1) Å, V = 3205.42(2) Å^3, Z = 4, D_{calcd} = 1.610 Mg m^{-3}, μ(Cu Kα) = 8.24 mm^{-1}, T = 150(2) K, yellow trapezoid, 0.31 x 0.25 x 0.16 mm, 6,486 independent reflections. F^2 refinement, R_1 = 0.029, wR_2 = 0.078 for 7,799 reflections (I > 2.0σ(I), $2\theta_{max}$ = 144°), 391 parameters, 0 restraints, CCDC 1881122.

Synthesis of [Ru(CO)(PMe_2Ph)(PPh_3){BH(mt)$_2$}] *(Ru→B)*[8] (13). A solution of [Ru(CO)(PPh_3)$_2${BH(mt)$_2$}] (**5**: 0.203 g, 0.23 mmol) and PMe_2Ph (0.10 mL, 0.70 mmol) in tetrahydrofuran (20 mL) was stirred for 4 h. The solvent was removed *in vacuo* to give an oily orange residue. Diethyl ether (20 mL) was added to afford a pale yellow solid that was isolated by cannula filtration. The solid was suspended in n-pentane and collected on a sinter funnel, washed with n-pentane, then dried under high vacuum. Yield: 0.059 g (0.077 mmol, 34%). IR (ATR, cm^{-1}): 3044 ν_{CH}, 2363 ν_{BH}, 1890 ν_{CO}. IR (THF, cm^{-1}): 2337 ν_{BH}, 1902 ν_{CO}. ^1H NMR (400 MHz, $CDCl_3$): δ_H = 1.28 (d, 3 H, $^2J_{HP}$ = 5.5, PCH_3), 1.43 (d, 3 H, $^2J_{HP}$ = 5.3, PCH_3), 3.00 (s, 3 H, NCH_3), 3.43 (s, 3 H, NCH_3), 6.19 (d, 2 H,

$^3J_{HH}$ = 2.6, NCH=CH), 6.60 (s, 2 H, NCH=CH), 7.07 – 7.13 (m, 9 H, C_6H_5), 7.30 – 7.52 (m, 14 H, C_6H_5). Decomposition in $CDCl_3$ confounded the acquirement of useful $^{13}C\{^1H\}$ NMR data. $^{31}P\{^1H\}$ NMR (162 MHz, $CDCl_3$): δ_P = 56.9 (d, $^1J_{PC}$ = 11.3, PPh_3), –17.2 (s.br., PMe_2Ph). $^{11}B\{^1H\}$ NMR (128 MHz, $CDCl_3$): δ_B = 5.13 (s.br.). ^1H NMR (400 MHz, CD_2Cl_2): δ_H = 1.25 (d, 3 H, $^2J_{HP}$ = 5.5, PCH_3), 1.38 (d, 3 H, $^2J_{HP}$ = 5.3, PCH_3), 2.97 (s, 3 H, NCH_3), 3.49 (s, 3 H, NCH_3), 6.19 (d, 1 H, $^3J_{HH}$ = 1.4, NCH=CH), 6.27 (s, 1 H, NCH=CH), 6.63 (d, 1 H, $^3J_{HH}$ = 1.5, NCH=CH), 6.67 (s, 1 H, NCH=CH), 7.07 – 7.16 (m, 9 H, C_6H_5), 7.31 – 7.48 (m, 14 H, C_6H_5). $^{31}P\{^1H\}$ NMR (162 MHz, CD_2Cl_2): δ_P = 56.2 (s.br., PMe_2Ph), –17.7 (s.br., PPh_3). ESI-MS(+) m/z: 769.1 $[M+H]^+$. Accurate mass: Found 769.1099 $[M+H]^+$, Calcd. for $C_{35}H_{38}ON_4{}^{11}BP_2S_2{}^{102}Ru$ 769.1093. Anal. Found: C, 55.29; H, 5.02; N, 7.13%. Calcd. for $C_{35}H_{37}BN_4OP_2RuS_2$: C, 54.76; H, 4.86; N, 7.30%.

Synthesis of [Ru(CO)(PMe_2Ph)$_2${BH(mt)$_2$}] *(Ru→B)*[8] (14). A solution of [Ru(CO)(PPh_3)$_2${BH(mt)$_2$}] (**5**: 0.200 g, 0.22 mmol) and PMe_2Ph (0.30 mL, 2.7 mmol) in tetrahydrofuran (20 mL) was heated under reflux for 18 h. The solvent was reduced to 3 mL and diethyl ether (10 mL) and n-pentane (15 mL) were added to afford a pale yellow solid that was isolated by cannula filtration and dried under high vacuum. Yield: 0.079 g (0.12 mmol, 55%). Crystals suitable for crystallographic analysis were obtained from slow evaporation of a concentrated solution of **14** in tetrahydrofuran/diethyl ether/n-pentane over one day. IR (ATR, cm^{-1}): 2298 ν_{BH}, 1877 ν_{CO}. IR (THF, cm^{-1}): 2323 ν_{BH}, 1902 ν_{CO}. ^1H NMR (700 MHz, $CDCl_3$): δ_H = 1.27 (d, 3 H, $^2J_{HP}$ = 8.6, PCH_3), 1.38 (d, 3 H, $^2J_{HP}$ = 5.0, PCH_3), 1.43 (d, 3 H, $^2J_{HP}$ = 5.4, PCH_3), 1.48 (d, 3 H, $^2J_{HP}$ = 8.4, PCH_3), 3.40 (s, 3 H, NCH_3), 3.44 (s, 3 H, NCH_3), 6.48 (d, 1 H, $^3J_{HH}$ = 1.6, NCH=CH), 6.53 (s, 1 H, NCH=CH), 6.58 (s, 1 H, NCH=CH), 6.65 (d, 1 H, $^3J_{HH}$ = 1.7, NCH=CH), 7.09 – 7.13 (m, 3 H, C_6H_5), 7.20 – 7.22 (m, 2 H, C_6H_5), 7.26 – 7.28 (m, 1 H, C_6H_5), 7.31 – 7.33 (m, 2 H, C_6H_5), 7.43 – 7.46 (m, 2 H, C_6H_5). $^{13}C\{^1H\}$ NMR (176 MHz, $CDCl_3$): δ_C = 15.6 (dd, $^1J_{CP}$ = 31.2, $^3J_{CP}$ = 3.3, PCH_3), 16.3 (d, $^1J_{CP}$ = 13.6, PCH_3), 18.6 (dd, $^1J_{CP}$ = 32.3, $^3J_{CP}$ = 4.2, PCH_3), 19.4 (d, $^1J_{CP}$ = 16.2, PCH_3), 34.1 (NCH_3), 34.1 (NCH_3), 120.6 (d, $^4J_{CP}$ = 8.4, NCH=CH) overlapping with 120.6 (d, $^4J_{CP}$ = 7.6, NCH=CH), 121.1 (NCH=CH), 121.5 (NCH=CH), 127.3 [d, $^{2,3}J_{CP}$ = 8.2, $C^{2,3,5,6}(C_6H_5)$, 128.0 [d, $^{2,3}J_{CP}$ = 7.7, $C^{2,3,5,6}(C_6H_5)$, 127.6 [$C^4(C_6H_5)$], 127.8 [$C^4(C_6H_5)$], 129.3 [d, $^{2,3}J_{CP}$ = 7.8, $C^{2,3,5,6}(C_6H_5)$, 129.7 [d, $^{2,3}J_{CP}$ = 11.4, $C^{2,3,5,6}(C_6H_5)$, 143.2 [dd, $^1J_{CP}$ = 35.1, $^3J_{CP}$ = 5.9, $C^1(C_6H_5)$, 143.3 [d, $^1J_{CP}$ = 20.7, $C^1(C_6H_5)$], 165.0 (d, $^3J_{CP}$ = 23.7, CS), 165.3 (d, $^3J_{CP}$ = 20.2, CS), 207.7 (dd, $^2J_{CP}$ = 15.5, $^2J_{CP}$ = 3.3, CO). ^{31}P NMR (283 MHz, $CDCl_3$): δ_P = 14.5 (m.br., coupling not resolved, PMe_2Ph *trans* to S), –16.4 (s.br., PMe_2Ph *trans* to B). $^{31}P\{^1H\}$ NMR (283 MHz, $CDCl_3$): δ_P = 14.5 (d, $^1J_{PC}$ = 12.3, PMe_2Ph *trans* to S), –16.4 (s.br., PMe_2Ph *trans* to B). ^{11}B NMR (128 MHz, $CDCl_3$): δB = 5.00 (s.br.). ESI-MS(+) m/z: 633.0 [M – B]+. Accurate mass: Found 1311.1317 [2M + Na]+, Calcd. for $C_{50}H_{66}{}^{11}B_2N_8O_2{}^{23}NaP_4S_4{}^{102}Ru_2$: 1311.1313. Anal. Found: C, 46.57; H, 5.28; N, 8.63%. Calcd. for $C_{25}H_{33}BN_4OP_2RuS_2$: C, 46.66; H, 5.17; N, 8.71%. *Crystal data for* $C_{25}H_{33}BN_4OP_2RuS_2$: M_w = 643.52, orthorhombic, *P*bca, *a* = 8.5565(1), *b* = 18.5822(2), *c* = 36.1544(3) Å, *V* = 5748.50(5) Å^3, *Z* = 8, D_{calcd} = 1.487 Mg m^{-3}, μ(Cu Kα) = 7.03 mm-1, *T* = 150(2) K, clear colourless block, 0.19 x 0.10 x 0.05 mm, 5,806 independent reflections. F^2 refinement, R_1 = 0.039, wR_2 = 0.098 for 5,659 reflections ($I > 2.0\sigma(I)$, $2\theta_{max}$ = 144°), 328 parameters, 0 restraints, CCDC 1881123.

Synthesis of [Ru(CO){$P(OMe)_3$}$_2${BH(mt)$_2$}] *(Ru→B)*[8] (15). A solution of [Ru(CO)(PPh_3)$_2${BH(mt)$_2$}] (**5**: 0.202 g, 0.22 mmol) and $P(OMe)_3$ (0.10 mL, 0.85 mmol) in tetrahydrofuran (20 mL) was stirred for 18 h. The solvent was removed in vacuo and diethyl ether (10 mL) and n-pentane (15 mL) were added to afford a pale yellow solid that was isolated by cannula filtration and dried under high vacuum. Yield: 0.041 g (0.067 mmol, 30%). Crystals suitable for crystallographic analysis were obtained from slow evaporation of a concentrated solution of **15** in chloroform/n-pentane over one day. IR (ATR, cm^{-1}): 2358 ν_{BH}, 1921 ν_{CO}. IR (THF, cm^{-1}): 2244 ν_{BH}, 1934 ν_{CO}. ^1H NMR (700 MHz, $CDCl_3$): δH = 3.49 (s, 3 H, NCH_3), 3.49 (s, 3 H, NCH_3), 3.56 (d, 9 H, $^3J_{HP}$ = 10.8, OCH_3), 3.67 (d, 9 H, $^3J_{HP}$ = 11.1, OCH_3), 6.62 (d, 2 H, $^4J_{HP}$ = 6.6, NCH=CH), 6.69 (dd, 2 H, $^4J_{HP}$ = 8.1, $^3J_{HH}$ = 1.8, NCH=CH). $^{13}C\{^1H\}$ NMR (176 MHz, $CDCl_3$): δ_C = 34.2 (NCH_3), 34.3 (NCH_3), 50.8 (br., P *trans* to B), 52.0 (d, $^2J_{CP}$ = 5.9, P *trans* to S), 120.9 (d, $^4J_{CP}$ = 4.2, NCH=CH), 121.0 (d, $^4J_{CP}$ = 4.1, NCH=CH), 121.5 (d, $^4J_{CP}$ = 1.2, NCH=CH), 121.6 (NCH=CH), 165.3 (d, $^3J_{CP}$ = 24.3, CS), 166.9 (d, $^3J_{CP}$ = 28.4, CS), 207.7 (dd, $^2J_{CP}$ = 18.8, $^2J_{CP}$ = 5.5, CO). $^{31}P\{^1H\}$ NMR (162 MHz, $CDCl_3$): δ_P = 151.1 (d, $^2J_{PP}$ = 19.4, P *trans* to S), 153.7 (s.br., P *trans* to B). ^{31}P NMR (162 MHz, $CDCl_3$): δ_P = 151.1 (m, $^2J_{PP}$ = 10.5, P *trans* to S), 153.7 (s.br., P *trans* to B). ^{11}B NMR (128 MHz, $CDCl_3$): δ_B = 3.62 (s.br.). $^{11}B\{^1H\}$ NMR (128 MHz, $CDCl_3$): δ_B = 3.80 (s.br.). ESI-MS(+) m/z: 617.0 $[M+H]^+$. Accurate mass: Found 617.0166 $[M+H]^+$, Calcd. For $C_{15}H_{29}{}^{11}BN_4O_7P_2S_2{}^{102}Ru$: 617.0162. Anal. Found: C, 29.35; H, 4.71; N, 8.98%. Calcd. for $C_{15}H_{29}BN_4O_7P_2RuS_2$: C, 29.28; H, 4.75; N, 9.10%. *Crystal data for* $(C_{15}H_{29}BN_4O_7P_2RuS_2)_3$: M_w = 1846.13, triclinic, *P*-1 (No.2), *a* = 9.4439(1), *b* = 15.2581(3), c = 26.4419(4) Å, α = 93.1670(14)°, β = 92.0931(12)°, γ = 93.9263(13)°, *V* = 3792.32(6) Å^3, *Z* = 2, D_{calcd} = 1.617 Mg m^{-3}, μ(Cu Kα) = 8.14 mm^{-1}, *T* = 150(2) K, colourless needles, 0.42 x 0.06 x 0.04 mm, 15,286 independent reflections. F^2 refinement, R_1 = 0.038, wR_2 = 0.098 for 13,859 reflections ($I > 2.0\sigma(I)$, $2\theta_{max}$ = 144°), 914 parameters, 0 restraints, CCDC 1881124.

Synthesis of [Ru(CO)(*Z*-$Ph_2PCH{=}CHPPh_2$){BH(mt)$_2$}] *(Ru→B)*[8] (16). A solution of [Ru(CO)(PPh_3)$_2${BH(mt)$_2$}] (**5**: 0.200 g, 0.22 mmol) and *Z*-$PPh_2CH{=}CHPPh_2$ (0.090 g, 0.22 mmol) in tetrahydrofuran (20 mL) was heated under reflux for 43 h. The solvent was removed *in vacuo* and diethyl ether was added to the orange residue to give a yellow solid that was isolated by cannula filtration. The solid was redissolved in tetrahydrofuran and layered with n-pentane. The filtrate was decanted to afford a yellow precipitate that was dried in air. Yield: 0.042 g (0.055 mmol, 24%). Crystals suitable for crystallographic analysis were obtained from vapour diffusion of n-pentane into a concentrated solution of **16** in acetone over one day. IR (ATR, cm^{-1}): 2354 ν_{BH}, 1905 ν_{CO} cm-1. IR (THF): 2338 ν_{BH}, 1923 ν_{CO}. ^1H NMR (700 MHz, $CDCl_3$): δ_H = 2.68 (s, 3 H, NCH_3), 3.55 (s, 3 H, NCH_3), 6.15 (s, 1 H, NCH=CH), 6.51 (s, 1 H, NCH=CH), 6.66 (s, 1 H, NCH=CH), 6.73 (s, 1 H, NCH=CH), 6.97 (m.br., 3 H, C_6H_5), 7.04 – 7.07 (m, 2 H, C_6H_5), 7.22 – 7.24 (m, 1 H, C_6H_5), 7.28 – 7.47 (m, 9 H, C_6H_5), 7.71 – 7.79 (m, 3 H, C_6H_5), 7.90 – 7.92 (m, 1 H, PCH=CHP), 7.97 – 7.99 (m, 1 H, PCH=CHP), 8.04 – 8.06 (m, 2 H,

C_6H_5). $^{13}C\{^1H\}$ NMR (151 MHz, $CDCl_3$): δ_C = 33.3 (NCH_3), 34.3 (NCH_3), 120.4 (NCH=CH) overlapping with 120.5 (d, $^4J_{CP}$ = 3.0, NCH=CH), 120.8 (d, $^4J_{CP}$ = 3.0, NCH=CH), 121.7 (NCH=CH), 125.7 [d, $^{2,3}J_{CP}$ = 9.6, $C^{2,3,5,6}(C_6H_5)$], 127.4 [$C^4(C_6H_5)$], 128.0 [d, $^{2,3}J_{CP}$ = 9.4, $C^{2,3,5,6}(C_6H_5)$], 128.4 [d, $^{2,3}J_{CP}$ = 8.8, $C^{2,3,5,6}(C_6H_5)$], 128.5 [d, $^{2,3}J_{CP}$ = 8.4, $C^{2,3,5,6}(C_6H_5)$], 128.7 [$C^4(C_6H_5)$], 129.4 [$C_4(C_6H_5)$], 129.6 [$C^4(C_6H_5)$], 131.1 [d, $^{2,3}J_{CP}$ = 8.5, $C^{2,3,5,6}(C_6H_5)$], 131.6 [d, $^{2,3}J_{CP}$ = 13.2, $C^{2,3,5,6}(C_6H_5)$], 133.0 [d, $^{2,3}J_{CP}$ = 14.6, $C^{2,3,5,6}(C_6H_5)$, 133.4 [d, $^{2,3}J_{CP}$ = 9.8, $C^{2,3,5,6}(C_6H_5)$, 135.5 [dd, $^1J_{CP}$ = 44.1, $^3J_{CP}$ = 4.5, $C^1(C_6H_5)$], 137.0 [d, $^1J_{CP}$ = 9.1, $C^1(C_6H_5)$], 137.2 [d, $^1J_{CP}$ = 16.2, $C^1(C_6H_5)$, 139.5 [d, $^1J_{CP}$ = 27.2, $C^1(C_6H_5)$, 148.1 [dd, $^1J_{CP}$ = 26.6, $^2J_{CP}$ = 26.6, PCH=CHP), 149.0 (dd, $^1J_{CP}$ = 35.8, $^2J_{CP}$ = 45.5, PCH=CHP), 164.5 (d, $^3J_{CP}$ = 22.7, CS), 166.1 (d, $^3J_{CP}$ = 19.6, $^3J_{CP}$ = 1.5, CS), 206.9 (d, $^2J_{CP}$ = 10.6, CO). $^{31}P\{^1H\}$ NMR (162 MHz, $CDCl_3$): δ_P = 70.6 (d, $^2J_{PP}$ = 8.1, P *trans* to S), 50.8 (s.br., P *trans* to B). ^{11}B NMR (128 MHz, $CDCl_3$): δ_B = 5.05 (s.br.). ESI-MS(+) m/z: 765.1 $[M+H]^+$. Accurate mass: Found 765.0785 $[M+H]^+$, Calcd. for $C_{35}H_{34}{}^{11}BN_4OP_2S_2{}^{102}Ru$ 765.0780. Anal. Found: C, 54.97; H, 4.30; N, 7.22%. Calcd. for $C_{35}H_{33}BN_4OP_2RuS_2$: C, 55.05; H, 4.36; N, 7.34%. *Crystal data for* $C_{35}H_{33}BN_4OP_2RuS_2$: M_w = 763.63, triclinic, *P*-1 (No.2), *a* = 10.4568(5), *b* = 12.4325(5), *c* = 15.9030(7) Å, α = 68.191(4)°, β = 82.434(4)°, γ = 71.916(4)°, *V* = 1824.35(8) Å^3, *Z* = 2, D_{calcd} = 1.390 Mg m^{-3}, μ(Cu Kα) = 5.64 mm^{-1}, *T* = 150(2) K, yellow block, 0.21 x 0.14 x 0.07 mm, 7,333 independent reflections. F^2 refinement, R_1 = 0.037, wR_2 = 0.101 for 6,926 reflections ($I > 2.0\sigma(I)$, $2\theta_{max}$ = 144°), 418 parameters, 0 restraints, CCDC 1881125.

Attempted synthesis of [Ru{κ³-*B,S,S'*-B(mt)$_2$}(CO)(PPh$_3$)$_2$]PF$_6$; Observation of [RuF(Hmt)$_2$(CO)(PPh$_3$)$_2$]PF$_6$ [11]PF$_6$. A solution of $[Ru(CO)(PPh_3)_2\{BH(mt)_2\}]$ (**5**: 0.100 g, 0.112 mmol) and $[CPh_3]PF_6$ (0.037 g, 0.095 mmol) in tetrahydrofuran (10 mL) was stirred for 24 h. The solvent was removed *in vacuo* and diethyl ether (10 mL) was added to afford an orange precipitate that was isolated *via* cannula filtration. Crude mixture: IR (THF, cm^{-1}): 1931 ν_{CO}, 1972 ν_{CO}. $^{31}P\{^1H\}$ NMR (162 MHz, C_6D_6): δ_P = 39.6 (s.br.), –142.9 (h, $^1J_{PF}$ = 713.9, PF_6), –5.3 (s.br., PPh_3). The orange precipitate had poor solubility in C_6D_6. $^{31}P\{^1H\}$ NMR (162 MHz, $CDCl_3$): δ_P = 43.8, 39.0 (s.br.), 35.3, 26.2, 24.9, –144.3 (h, $^1J_{PF}$ = 714.7, PF_6), –5.3 (PPh_3). Crystals of $[RuF(Hmt)_2(CO)(PPh_3)_2]PF_6$ [**11**]PF_6 suitable for crystallographic analysis were obtained from slow evaporation of a concentrated solution of the crude reaction mixture in benzene/n-pentane over one day. *Crystal data for* $C_{45}H_{42}FN_4OP_2RuS_2.F_6P.C_6H_6$: M_w = 1124.03, monoclinic, $P2_1/c$, *a* = 14.5664(1), *b* = 15.1058(1), *c* = 23.6542(2) Å, *V* = 5016.47(7) Å^3, *Z* = 4, D_{calcd} = 1.488 Mg m^{-3}, μ(Cu Kα) = 4.80 mm^{-1}, *T* = 150(2) K, yellow block, 0.18 x 0.11 x 0.07 mm, 10,144 independent reflections. F^2 refinement, R_1 = 0.044, wR_2 = 0.104 for 9,278 reflections ($I > 2.0\sigma(I)$, $2\theta_{max}$ = 144°), 729 parameters, 96 restraints, CCDC 1881121.

Acknowledgements

This work was supported by the Australian Research Council (DP170102695). The authors declare no conflicts of interest.

Notes and references

1 (a) A. F. Hill, G. R. Owen, A. J. P. White and D. J. Williams, *Angew. Chem., Int. Ed*., 1999, **38**, 2759 – 2761. (b) I. R. Crossley, M. R. St.-J. Foreman, A. F. Hill, G. R. Owen, A. J. P. White, D. J. Williams and A. C. Willis, *Organometallics*, 2008, **27**, 381 – 386. (c) M. R. St.-J. Foreman, A. F. Hill, G. R. Owen, A. J. P. White and D. J. Williams, *Organometallics*, 2003, **22**, 4446 – 4450.

2 For reviews see: (a) H. Braunschweig and R. D. Dewhurst, *Dalton Trans.*, 2011, **40**, 549 – 558. (b) A. Amgoune and D. Bourissou, *Chem. Commun.*, 2011, **47**, 859 – 871. (c) G. Bouhadir and D. Bourissou, *Chem. Soc. Rev.,* 2016, **45**, 1065 – 1079. (d) G. R. Owen, *Chem. Soc. Rev.,* 2012, **41**, 3535 – 3546.

3 H. C. Brown and E. A. J. Fletcher, *J. Am. Chem. Soc.*, 1951, **73**, 2808 – 2813.

4 A. Haarland, *Angew. Chem. Int. Ed.*, 1989, **28**, 922 – 1007

5 Herein we consider the borane cage in metallaboratranes to be neutral BR_3 units such that complexes such as **1** are deemed to be zerovalent. For further discussions on oxidation state and d^n assignments for metallaboratranes see (a) A. F. Hill, *Organometallics*, 2006, **25**, 4741 – 4743. (b) G. Parkin, *Organometallics*, 2006, **25**, 4744 – 4747.

6 (a) M. R. St.-J. Foreman, A. F. Hill, A. J. P. White and D. J. Williams, *Organometallics*, 2004, **23**, 913 – 916. (b) I. R. Crossley, M. R. St.-J. Foreman, A. F. Hill, A. J. P. White and D. J. Williams, *Chem. Commun.*, 2005, 221 – 223. (c) I. R. Crossley, A. F. Hill, E. R. Humphrey and A. C. Willis, *Organometallics*, 2005, **24**, 4083 – 4086. (d) I. R. Crossley and A. F. Hill, *Organometallics*, 2004, **23**, 5656 – 5658. (e) D. J. Mihalcik, J. L. White, J. M. Tanski, L. N. Zakharov, G. P. A. Yap, C. D. Incarvito, A. L. Rhenigold and D. Rabinovich, *Dalton Trans*., 2004, 1626 – 1634. (f) H. Zhu, Q. Ma, A.-Q. Jia, Q. Chen, W.-H. Leung and Q.-F. Zhang, *Inorg. Chim. Acta*, 2013, **405**, 427 – 436. (g) R. J. Blagg, J. P. H. Charmant, N. G. Connelly, M. F. Haddow and A. Guy Orpen, *Chem. Commun.*, 2006, 2350 – 2352. (h) R. J. Blagg, C. J. Adams, J. P. H. Charmant, N. G. Connelly, M. F. Haddow, A. Hamilton, J. Knight, A. G. Orpen and B. M. Ridgeway, *Dalton Trans.*, 2009, 8724 – 8736. (i) M. J. López-Gómez, N. G. Orpen, M. F. Haddow, A. Hamilton and A. G. Orpen, *Dalton Trans.*, 2010, **39**, 5221 – 5230. (j) R. J. Blagg, N. G. Connelly, M. F. Haddow, A. Hamilton, M. Lusi, A. G. Orpen and B. M. Ridgeway, *Dalton Trans.*, 2010, **39**, 11616 – 11627. (k) G. R. Owen, P. H. Gould, J. P. H. Charmant, A. Hamilton and S. Saithon, *Dalton Trans.*, 2010, **39**, 392 – 400. (l) N. Tsoureas, T. Bevis, C. P. Butts, A. Hamilton and G. R. Owen, *Organometallics*, 2009, **28**, 5222 – 5232. (m) G. R. Owen, P. H. Gould, A. Hamilton and N. Tsoureas, *Dalton Trans.*, 2010, **39**, 49 – 52. (n) A. Zech, M. F. Haddow, H. Othman and G. R. Owen, *Organometallics*, 2012, **31**, 6753 – 6760. (o) S. Holler, M. Tüchler, A. M. Knaus, F. Belaj, N. C. Mösch-Zanetti, *Polyhedron*, 2017, **125**, 122 – 129. (p) G . Nuss, G. Saischek, B. N. Harum, M. Volpe, K. Gatterer, F. Belaj and N. C. Mösch-Zanetti, *Inorg. Chem.*, 2011, **50**, 1991 – 2001. (q) S. Holler, M. Tüchler, F. Belaj, L. F. Veiros, K. Kirchner and N. Mösch-Zanetti, *Inorg. Chem.*, 2016, 55, 4980 – 4991. (r) S. Holler, M. Tüchler, M. C. Roschger, F. Belaj, L. F. Veiros, K. Kirchner and N. C. Mösch-Zanetti, *Inorg. Chem.*, 2017, **56**, 12670 – 12673. (s) G. Nuss, G. Saischek, B. N. Harum, M. Volpe, F. Belaj and N. C. Mösch-Zanetti, *Inorg. Chem.*, 2011, 50, 12632 – 12640. (t) S. Senda, Y. Ohki, T. Hirayama, D. Toda, J.-L. Chen, T. Matsumoto, H. Kawaguchi and K. Tatsumi, *Inorg. Chem.*, 2006, **24**, 9914 – 9925.

7 (a) S. Bontemps, H. Gornitzka, G. Bouhadir, K. Miqueu and D. Bourissou, *Angew. Chem., Int. Ed.,* 2006, **45**, 1611 – 1614. (b) S. Bontemps, G. Bouhadir, P. W. Dyer, K. Miqueu, D. Bourissou, *Inorg. Chem.*, 2007, **46**, 5149 – 5151 (c) S. Bontemps, M. Sircoglou, G. Bouhadir, H. Puschmann, J. A. K. Howard, P. W. Dyer, K. Miqueu and D. Bourissou, *Chem.-Eur.*

J., 2008, **14**, 731 – 740. (d) M. Sircoglou, S. Bontemps, M. Mercy, N. Saffon, M. Takahashi, G. Bouhadir, L. Maron and D. Bourissou, *Angew. Chem., Int. Ed.,* 2007, **46**, 8583– 8586.

8 M. R. St.-J. Foreman, A. F. Hill, C. Ma, N. Tshabang and A. J. P. White, *Dalton Trans.,* in press, doi:10.1039/c8dt04278k.

9 J.G. Verkade, *Coord. Chem. Rev*., 1994, **137**, 233 – 295.

10 (a) J. J. Molloy and A. B. Watson, *ACS Symposium Series*, 2016, **1236**, 379 – 413. (b) J. W. B. Fyfe and A. B. Watson, **Synlett**, 2015, **26**, 1139 – 1144

11 (a) I. R. Crossley, A. F. Hill and A. C. Willis, *Organometallics,* 2010, **29**, 326– 336. (b) I. R. Crossley, A. F. Hill and A. C. Willis, *Organometallics*, 2005, **24**, 1062 – 1064. (c) D. K. Roy, K. Yuvaraj, R. Jagan and S. Ghosh, *J. Organomet. Chem.*, 2016, **811**, 8 – 13. (d) R. S. Anju, D. K. Roy, B. Mondal, K. Yuvaraj, C. Arivazhagan, K. Saha, B. Varghese and S. Ghosh, *Angew. Chem., Int. Ed.,* 2014, **53**, 2873– 2877. (e) A. Zech, M. F. Haddow, H. Othman and G. R. Owen, *Organometallics*, 2012, **31**, 6753 – 6760. (f) N. Tsoureas, A. Hamilton, M. F. Haddow, J. N. Harvey, A. G. Orpen and G. R. Owen, *Organometallics*, 2013, **32**, 2840– 2856. (g) D. K. Roy, A. De, S. Panda, B. Varghese and S. Ghosh, *Chem. Eur. J.*, 2015, **21**, 13732– 13738. (h) G. Dyson, A. Zech, B. W. Rawe, M. F. Haddow, A. Hamilton and G. R. Owen, *Organometallics*, 2011, **30**, 5844– 5850. (i) A. Neshat, H. R. Shahsavari, P. Mastrorilli, S. Todisco, M. G. Haghaghi and B. Notash, *Inorg. Chem.,* 2018, **57**, 1398 – 1407.

12 (a) D. L. M. Suess and J. C. Peters, *J. Am. Chem. Soc.*, 2013, **135**, 12580 – 12583. (b) M. A. Nesbit, D. L. M. Suess and J. C. Peters, *Organometallics*, 2015, **34**, 4741 – 4752. (c) W. H. Harman and J. C. Peters, *J. Am. Chem. Soc.*, 2012, **134**, 5080– 5082.(d) W. H. Harman, T.-P. Lin and J. C. Peters, *Angew. Chem., Int. Ed.,* 2014, **53**, 1081– 1086. (e) D. L. M. Suess and J. C. Peters, *J. Am. Chem. Soc.*, 2013, **135**, 4938 – 4941. (f) D. L. M. Suess, C. Tsay and J. C. Peters, *J. Am. Chem. Soc.*, 2012, **134**, 14158 – 14164. (g) H. Kameo and H. Nakazawa, *Organometallics*, 2012, **31**, 7476– 7484. (h) C. M. Conifer, D. J. Law, G. J. Sunley, A. J. P. White and G. J. P. Britovsek, *Organometallics*, 2011, **30**, 4060 – 4066. (i) W.-C. Shih, W. Gu, M. C. MacInnis, D. E. Herbert and O. V. Ozerov, *Organometallics*, 2017, **36**, 1718– 1726. (j) B. E. Cowie, D. J. H. Emslie, H. A. Jenkins, and J. F. Britten, *Inorg. Chem.*, 2010, **49**, 4060 – 4072. (k) D. Schuhknecht, F. Ritter and M. E. Tauchert, *Chem. Commun*., 2016, **52**, 11823– 11826. (l) P. Steinhoff and M. E. Tauchert, *Beilstein J. Org. Chem.*, 2016, **12**, 1573 – 1576. (m) B. E. Cowie and D. J. H. Emslie, *Chem. Eur. J.*, 2014, **20**, 16899– 16912. (n) T. Schindler, M. Lux, M. Peters, L. T. Scharf, H. Osseili, L. Maron and M. E. Tauchert, *Organometallics*, 2015, **34**, 1978 – 1984. (o) F. Inagaki, C. Matsumoto, Y. Okada, N. Maruyama and C. Mukai, *Angew. Chem., Int. Ed.*, 2015, **54**, 818 – 822.

13 (a) G. R. Owen, P. H. Gould, A. Hamilton and N. Tsoureas, *Dalton Trans.*, 2010, **39**, 49 – 52. (b) N. Tsoureas, Y.-Y. Kuo, M. F. Haddow and G. R. Owen, *Chem.Commun.*, 2011, **47**, 484 – 486. (c) M. J. Lopez-Gomez, N. G. Connelly, M. F. Haddow, A. Hamilton, M. Lusi, U. Baisch and A. G. Orpen, *Dalton Trans.,* 2011, **40**, 4647 – 4659. (d) V. K. Landry, J. G. Melnick, D. Buccella, K. Pang, J. C. Ulichny and G. Parkin, *Inorg. Chem.,* 2006, **45**, 2588– 2597. (e) K. Pang, S. M. Quan and G. Parkin, *Chem. Commun.*, 2006, 5015– 5017. (f) N. Tsoureas, M. F. Haddow, A. Hamilton and G. R. Owen, *Chem. Commun.*, 2009, 2538 – 2540.

14 I. R. Crossey, A. F. Hill and A. C. Willis, *Organometallics*, 2007, **26**, 3891 – 3895.

15 (a) C. E. F. Rickard, W. R. Roper, G. E. Taylor, J. M. Waters and L. J. Wright, *J. Organomet. Chem.* **1990**, *389*, 375. (b) D. S. Bohle, G. R. Clark, C. E. F. Rickard, W. R. Roper and L. J. Wright, *J. Organomet. Chem.* **1988**, *358*, 442

16 M. R. Torres, A. Vegas, A. Santos and J. Ros, *J. Organomet. Chem.* **1986**, *309*, 169.

17 M. R. St.-J. Foreman, A. F. Hill, N. Tshabang, A. J. P. White and D. J. Williams, *Organometallics,* 2003, **22**, 5593 – 5596.

18 M. R. St.-J. Foreman, C. Ma, A. F. Hill, N. E. Otten, M. Sharma, N. Tshabang and J. S. Ward, *Dalton Trans.*, 2017, **46**, 14957 – 14972.

19 (a) S. L. Kuan, W. K. Leong, R. D. Webster, L. Y. Goh, *Organometallics,* 2012, **31**, 5159 - 5168. (b) G. C. Rudolf, A. Hamilton, A. G. Orpen, G. R. Owen *Chem. Commun.* 2009, 553 – 555. (c) H. Zhu, Q. Ma, A.-Q. Jia, Q. Chen, W.-H. Leung, Q.-F. Zhang, *Inorg. Chim. Acta* 2013, **405**, 427 – 436. (d) D. K. Roy, B. Mondal, R. S. Anju, S. Ghosh *Chem. Eur. J.* 2015, **21**, 3640 – 3648. (e) Q. Ma, A.-Q. Jia, Q. Chen, H.-T. Shi, W.-H. Leung, Q.-F. Zhang *J. Organomet. Chem.* 2012, **716**, 182 – 186. (f) M. Jimenez-Tenorio, M. C. Puerta, P. Valerga *Organometallics* 2009, **28**, 2787 – 2798. (g) X.-Y. Wang, Q. Ma, T. Duan, Q. Chen, Q.-F. Zhang *Inorg. Chim. Acta* 2012, **384**, 281 – 286. (h) S. L. Kuan, W. K. Leong, L. Y. Goh, R. D. Webster *J. Organomet. Chem.* 2006, **691**, 907 – 915. (i) X.-Y. Wang, H.-T. Shi, F.-H. Wu, Q.-F. Zhang *J. Mol. Struct.* 2010, **982**, 66 – 72. (j) R. Rajasekharan-Nair, L. Darby, J. Reglinski, M. D. Spicer, A. R. Kennedy *Inorg. Chem. Commun*. 2014, **41**, 11 – 13. (k) R. J. Abernethy, A. F. Hill, N. Tshabang, A. C.Willis, R. D. Young *Organometallics* 2009, **28**, 488 – 492.

20 For electronic book-keeping purposes the line formula $(M{\rightarrow}B)^x$ addendum allocates a total of x d-electrons to the metal including the pair involved in the metal-boron dative bond.

21 J. D. E. T. Wilton-Ely, S. J. Honarkhah, M. Wang, D. Tocher and A. M. Z. Slawin, *Dalton Trans.* **2005**, 1930 – 1939.

22 I. R. Crossley, A. F. Hill and A. C. Willis, *Organometallics*, 2006, **25**, 289 – 299.

23 I. R. Crosley, A. F. Hill and A. C. Willis, *Organometallics*, 2008, **27**, 312 – 315.

24 J. S. Figueroa, J. G. Melnick and Gerard Parkin, *Inorg. Chem.*, 2006, **45**, 7056 – 7058.

25 (a) C. Bianchini, M. Peruzzini, F. Zanobini, P. Frediani and A. Albinati, *J. Am. Chem. Soc.*, 1991, **113**, 5453 – 5454. (b) M. Bassetti, S. Marini, F. Tortorella, V. Cadierno, J. Diez, M. P. Gamasa and J. Gimeno, *J. Organomet. Chem.*, 2000, **593 – 594**, 292 – 298. (c) S. Pavlik, C. Gemel, C. Slugovc, K. Mereiter, R. Schmid and K. Kirchner, *J. Organomet. Chem.*, 2001, **617 – 618**, 301 – 310. (d) R. R. Kirss, R. D. Ernst and A. M. Arif, *J. Organomet. Chem.*, 2004, **689**, 419 – 428. (e) H. Katayama and F. Ozawa, Fumiyuki, *Coord. Chem. Rev.*, 2004, **248**, 1703 – 1715. (f) J.-H. Lee and K. G. Caulton, *J. Organomet. Chem.*, 2008, **693**, 1664 – 1673. (g) M. Jimenez-Tenorio, C. M. Puerta and P. Valerga, *Organometallics*, 2009, **28**, 2787 – 2798.

26 (a) A. F. Hill and R. P. Melling, *J. Organomet. Chem.*, 1990, **396**, C22 - C24. (b) A. F. Hill, R. P. Melling and A. R. Thompsett, *J. Organomet. Chem.*, 1991, **402**, C8 – C11. (c) A. F. Hill, M. C. J. Harris and R. P. Melling, *Polyhedron*, 1992, **11**, 781 – 787

27 A. M. Echavarren, J. López, A. Santos and J. Montoya, *J. Organomet. Chem.* 1991, **414**, 393.

28 I. R. Crossley and A. F. Hill, *Dalton Trans.* 2008, 201 – 203.

29 (a) Y. Qin, Q. Ma, A.-Q. Jia, Q. Chen and Q.-F. Zhang, *J. Coord. Chem.* 2013, **66**, 1405 – 1415. (b) D. Taher, M. Al-Noaimi, S. Mohammad, J. F. Corrigan, D. G. MacDonald and M. El-Khateeb, *Inorg. Chim. Acta* 2010, **363**, 4134 – 4139. (c) S. Parsons, F. Mclachlan, P. Bailey, J. Davidson and R. Johnstone, *CCDC Communication (Private Communication)* 2006.

30 K. Pang, J. M. Tanski and G. Parkin, *Chem. Commun.,* 2008, 1008 – 1010.

31 (a) S. A. Brewer, K. S. Coleman, J. Fawcett, J. H. Holloway, E. G. Hope, D. R. Russell and P. G. Watson, *J. Chem. Soc., Dalton Trans.,* 1995, 1073 – 1076. (b) S. P. Reade, D. Nama, M. F. Mahon, P. S. Pregosin and M. K. Whittlesey, *Organometallics* **2007**, *26*, 3484 – 3491.

32 Although Karplus curves relating $^3J_{PC}$ to C–P–Ru-P dihedral angles are not available, the angular dependence of vicinal couplings for P–Ru–S–H and P–Ru–P–H connectivities have been discussed (a) M. Karplus*, J. Chem. Phys.,* 1959, **30**, 11 –

15. (b) E. S. F. Ma, S. J. Rettig and B. R. James, *Chem. Commun*., 2463 – 2464. (c) V. K. Greenacre, I. J. Day and I. R. Crossley, *Organometallics*, 2017, **36**, 435 – 442.
33 (a) Y. Gloaguen, G. Alcaraz, A.-F. Pecharman, E. Clot, L. Vendier and S. Sabo-Etienne, *Angew. Chem., Int. Ed.*, 2009, **48**, 2964 – 2968. (b) K. Namura and H. Suzuki, *Organometallics*, 2014, **33**, 2968 – 2983.
34 T. Saito, S. Kuwata and T. Ikariya, *Chem. Lett.* **2006**, *35*, 1224 – 1225.
35 K. R. Grundy, R. O. Harris and W. R. Roper*, J. Organomet. Chem.*, 1975, **90**, C34 – C36.
36 C. A. Tolman, *Chem. Rev.*, 1977, **77**, 313 –348.
37 M. Sircoglou, S. Bontemps, G. Bouhadir, N. Saffon, K. Miqueu, W. Gu, M. Mercy, C.-H. Chen, B.-M. Foxman, L. Maron, O. V. Ozerov and D. Bourissou, *J. Am. Chem. Soc.* **2008**, *130*, 16729 – 16738.
38 (a) P. C. Ray and N. K. Dutt, *J. Indian. Chem. Soc.*, 1943, **20,** 81 – 92. (b) J. C. Bailar Jr., *J. Inorg. Nucl. Chem.,* 1958, **8**, 165 – 175. (c) A. Rodger and B. F. G. Johnson, *Inorg. Chem*., 1988, **27**, 3062 – 3064. (d) H. S. Rzepa and M. E. Cass, *Inorg. Chem.*, 2007, **46**, 8024 – 8031. (e) G. E. Ball and B. E. Mann, *J. Chem. Soc., Chem. Commun.,* 1992, 561 – 563.
39 M. L. H. Green, *J. Organomet. Chem.,* 1995, **500**, 127 – 148.

Table of Contents Graphic